

March 2007  
DAMTP-  
hep-th/yymmnnn

## Giant Magnons and Singular Curves

Benoît Vicedo

DAMTP, Centre for Mathematical Sciences  
University of Cambridge, Wilberforce Road  
Cambridge CB3 0WA, UK

### Abstract

We obtain the giant magnon of Hofman-Maldacena and its dyonic generalisation on  $\mathbb{R} \times S^3 \subset AdS_5 \times S^5$  from the general elliptic finite-gap solution by degenerating its elliptic spectral curve into a singular curve. This alternate description of giant magnons as finite-gap solutions associated to singular curves is related through a symplectic transformation to their already established description in terms of condensate cuts developed in hep-th/0606145.

## 0 Introduction

Recently, a certain limit of the AdS/CFT correspondence was proposed by Hofman and Maldacena [1] in which the 't Hooft coupling  $\lambda$  is held fixed allowing for a direct interpolation between the gauge theory ( $\lambda \ll 1$ ) and string theory ( $\lambda \gg 1$ ). In the Hofman-Maldacena (HM) limit, the energy  $E$  (or conformal dimension  $\Delta = E$ ) and a  $U(1)$  R-charge  $J_1$  both become infinite with the difference  $E - J_1$  held fixed. On the string side, using static gauge  $X_0 = \kappa\tau$ , the energy density  $\mathcal{E} = \sqrt{\lambda}\kappa/2\pi$  is uniform along the string so that the string effectively becomes infinitely long in this limit. Likewise on the gauge side, the dual single-trace conformal operator of the form  $\text{tr}(Z^{J_1}W^{J_2})$  clearly becomes infinitely long in this limit. If we relax the trace condition then we are able to consider elementary excitations on the gauge side given by infinitely long operators of the form

$$\mathcal{O}_{\mathbf{p}} = \sum_l e^{i\mathbf{p}l} (\dots ZZZW \underset{\uparrow}{\phantom{W}} ZZZ \dots). \quad (0.1)$$

The trace condition is equivalent to the requirement that the total momentum of all excitations should vanish. The single excitation (0.1), which violates the momentum condition, describes a ‘magnon’ of momentum  $\mathbf{p}$  with dispersion relation [2, 3, 4, 5, 6]

$$E - J_1 = \sqrt{1 + \frac{\lambda}{\pi^2} \sin^2 \frac{\mathbf{p}}{2}}.$$

At large  $\lambda$  this state is described by a classical string solution on the real line called a ‘giant magnon’ which was identified in [1]. It corresponds to a solitonic solution of the infinite string embedded in an  $\mathbb{R} \times S^2$  subsector of  $AdS_5 \times S^5$ .

Subsequently, solitonic solutions of the infinite string moving through  $\mathbb{R} \times S^3$  referred to as ‘dyonic giant magnons’ were identified in [2] and constructed in [7]. These solutions carry an extra finite  $U(1)$  R-charge  $J_2$  and have the following dispersion relation

$$E - J_1 = \sqrt{J_2^2 + \frac{\lambda}{\pi^2} \sin^2 \frac{\mathbf{p}}{2}}.$$

They correspond on the gauge side to bound states of  $J_2$  magnons given by infinitely long operators of the form

$$\mathcal{O}_{\mathbf{p}} = \sum_l e^{i\mathbf{p}l} (\dots ZZZW \underset{\uparrow}{\phantom{W}}^{J_2} ZZZ \dots).$$

A general description of such dyonic giant magnons was then proposed in [8] using the language of finite-gap solutions and spectral curves [9, 10, 11, 12, 13], still restricting attention to the  $\mathbb{R} \times S^3$  sector. In this framework, every solution is characterised by a spectral curve  $\Sigma$  equipped with an Abelian integral  $p$  called the quasi-momentum, such that the pair  $(\Sigma, dp)$  encodes the integrals of motion of the solution. A single dyonic giant magnon can

be described by a condensate cut  $\mathcal{B}_1$  from  $x_1$  to  $\bar{x}_1$  on the spectral curve [8], whose presence can be traced down to the existence of a nonvanishing  $a$ -period for the differential of the quasi-momentum

$$\int_a dp \in 2\pi\mathbb{Z}.$$

The ensuing multivaluedness of the Abelian integral  $p(x)$  can equivalently be described in terms of simple poles of  $p(x)$  at the end points  $x_1, \bar{x}_1$  of each condensate cut  $\mathcal{B}_1$ . However, this new feature of the quasi-momentum, which was shown in [8] to correctly account for dyonic giant magnon solutions in the  $J_1 \rightarrow \infty$  limit, does not appear in the context of finite-gap integration simply because the  $a$ -periods of the differential  $dp$  can always be removed by appropriately normalising  $dp$  [9]. This apparent dilemma is resolved by noting that the general finite-gap solution to the equations of a closed string moving through  $\mathbb{R} \times S^3$ , constructed in [14, 15], are valid for all values of the R-charges  $J_1$  and  $J_2$ . It therefore ought to be possible to obtain dyonic giant magnon solutions as a special limit of finite-gap solutions when  $J_1 \rightarrow \infty$ , and in particular recover the condensate cut representation of [8] in this limit.

In a more recent paper [16], a family of solutions to the string equations of motion on  $\mathbb{R} \times S^3$  was found by exploiting its connection with the complex sine-Gordon model via Pohlmeyer's reduction. These solutions nicely interpolate between folded/circular strings on the one hand and dyonic giant magnons on the other, the latter being obtained in the  $J_1 \rightarrow \infty$  limit. The analytic form of these solutions, involving ratios of elliptic  $\Theta$ -functions and an overall exponential both of which exhibit a linear  $(\sigma, \tau)$ -dependence, is very reminiscent of the general finite-gap solution for a closed string moving on  $\mathbb{R} \times S^3$  constructed in [14, 15].

The aim of this paper is to identify the precise way in which finite-gap solutions degenerate into dyonic giant magnon solutions on the real line when taking the  $J_1 \rightarrow \infty$  limit. Inspired by the results of [16] we achieve this by first showing that the (type (i)) helical solutions with two spins of [16] are exactly elliptic finite-gap solutions of [14, 15]. The  $J_1 \rightarrow \infty$  limit of these solutions is then reinterpreted in the language of spectral curves. We find that dyonic giant magnons are obtained by degeneration of the spectral curve  $\Sigma$ , underlying the elliptic finite-gap solution, into a singular curve. In particular, the HM limit can be succinctly summed up as the limit where the modulus  $k$  of the elliptic curve  $\Sigma$  goes to unity. This corresponds to shrinking the real homology period of  $\Sigma$  (e.g. the  $b$ -period if the cycles are chosen such that  $\hat{\tau}b = b$ ).

In a general integrable 2-d field theory there is a well known connection between solutions to soliton equations on the line and finite-gap solutions on the circle [17]. The former can be described as a limit where the spectral curve of the latter becomes singular. This phenomenon has been studied in the case of the KdV and non-linear Schrödinger equations as well as other specific integrable field theories [18]. The present paper is the first step towards an investigation of such a connection in the case of the string equations of motion on  $\mathbb{R} \times S^3$ . In the pair of papers [19, 20], a way of constructing a generic configuration of

giant magnons for the equations of motion of the infinite string on  $\mathbb{R} \times S^5$  was presented which makes use of the dressing method for solitons. The subset of these solutions on  $\mathbb{R} \times S^3$  should be intimately related to singular limits of the general finite-gap solution constructed in [14, 15] by an extension of the singularisation procedure, which we identify in the present paper, to higher genus finite-gap solutions. We hope to come back to this issue soon [21]. Moreover, in the general theory of integrable 2-d field theories it is possible to apply this singularisation procedure only partially to the curve  $\Sigma$  (i.e. where only certain cuts are shrunk to singular points) which generally leads to more solutions describing solitons scattering on the background of a finite-gap solution. We do not yet fully understand the relevance of such partial degenerations in the present context of string theory on  $\mathbb{R} \times S^3$ , but hope to come back to this point in [21].

An investigation of finite-size corrections to giant magnons was initiated in [22]. There, a particular one-soliton solution describing a finite  $J_1$  magnon was considered. Given that giant magnons can be obtained as degenerations of finite-gap solutions in the  $J_1 \rightarrow \infty$  limit, which are valid for arbitrary values of  $J_1, J_2$ , we propose that finite-gap solutions should provide the general finite-size corrections to giant magnons.

The paper is organised as follows. In section 1 we recall the construction of the general finite-gap solution to the equations of a string on  $\mathbb{R} \times S^3$  [14, 15]. In section 2 we restrict attention to the elliptic finite-gap solution and explicitly express every ingredient in the solution in terms of elliptic integrals and elliptic functions, reducing any integral to the standard elliptic integrals of the first, second and third kind. As a result, the general elliptic finite-gap solution is shown to be equivalent to the (type (i)) helical solution of [16]. Using this general two-cut solution, in section 3 we identify the nature of the HM limit in the finite-gap language. We also reconcile this picture of dyonic giant magnons as singular limits of finite-gap solutions with their description in terms of condensate cuts. Details of the calculations in section 2 are relegated to a series of four appendices.

## 1 Finite-gap string on $\mathbb{R} \times S^3$

The starting point for the method of finite-gap integration is to rewrite the equations of motion

$$d * j = 0, \quad dj - j \wedge j = 0, \quad j \in \mathfrak{su}(2)$$

which should be supplemented by the Virasoro constraints  $\frac{1}{2} \text{tr } j_{\pm}^2 = -\kappa^2$  (working in conformal static gauge), as the flatness condition

$$dJ(x) - J(x) \wedge J(x) = 0, \tag{1.1}$$

for the Lax connection  $J(x) = \frac{j - x * j}{1 - x^2} \in \mathfrak{sl}(2, \mathbb{C})$ , which depends on the spectral parameter  $x \in \mathbb{C}$ . The flatness (1.1) of the current  $J(x)$  immediately allows one to construct an infinite

number of conserved quantities for the string, which can be neatly encoded in the spectral curve

$$\Gamma : \quad \Gamma(x, y) = \det(y\mathbf{1} - \Omega(x, \sigma, \tau)) = 0,$$

where the monodromy matrix  $\Omega(x, \sigma, \tau) = P \overleftarrow{\exp} \int_{[c_{\sigma, \tau}]} J(x) \in SL(2, \mathbb{C})$  is one of the principal objects in integrable field theories. A non-singular version of this curve can be obtained, which we henceforth call  $\Sigma$ . For generic values of  $x$  the monodromy matrix  $\Omega(x, \sigma, \tau)$  has two distinct eigenvalues, and hence the curve  $\Gamma$  (or  $\Sigma$ ) is a double sheeted ramified cover of  $\mathbb{CP}^1$  with hyperelliptic projection  $\hat{\pi} : \Sigma \rightarrow \mathbb{CP}^1, P \mapsto x$ ; we define the notation  $\{x^\pm\} = \hat{\pi}^{-1}(x)$  for the set of points above  $x \in \mathbb{CP}^1$ . The hyperelliptic curve  $\Sigma$  is equipped with a hyperelliptic holomorphic involution  $\hat{\sigma} : \Sigma \rightarrow \Sigma$  which exchanges the two sheets  $\hat{\sigma}(x^\pm) = x^\mp$  as well as an anti-holomorphic involution  $\hat{\tau} : \Sigma \rightarrow \Sigma$  which maps both sheets to themselves by  $x \mapsto \bar{x}$  and derives from reality conditions on  $\Omega(x, \sigma, \tau)$  [14]. In this setup, the dynamical variables are described by a line bundle

$$L_{\sigma, \tau} \rightarrow \Sigma$$

which encodes the eigenvector  $\psi(P), P \in \Sigma$  of  $\Omega(x, \sigma, \tau)$ . Thus every solution  $j$  of the equations of motion specifies a unique curve  $\Sigma$  and line bundle  $L_{\sigma, \tau}$  over this curve; we shall assume that  $\Sigma$  has finite-genus in which case the solution  $j$  from which it originates is called a *finite-gap solution*. Now equation (1.1) is the consistency condition of the auxiliary linear problem

$$(d - J(x))\psi = 0, \tag{1.2}$$

so that (1.2) admits a solution for  $\psi(P)$  only if  $J(x)$  satisfies (1.1). The main idea of the method of finite-gap integration is to note that  $\psi(P)$  is uniquely specified by its analytic properties in  $P \in \Sigma$  which can be read off from (1.2), (these properties define what is called a Baker-Akhiezer vector on  $\Sigma$  relative to the data  $\{\hat{\gamma}, s_\pm\}$ )

$$\begin{aligned} (\psi_1) &\geq \hat{\gamma}^{-1} \infty^-, \quad \psi_1(\infty^+) = 1, \quad \text{and} \quad (\psi_2) \geq \hat{\gamma}^{-1} \infty^+, \quad \psi_2(\infty^-) = 1, \\ \text{with} \quad &\begin{cases} \psi_i(x^\pm, \sigma, \tau) e^{\mp s_+(x, \sigma, \tau)} = O(1), & \text{as } x \rightarrow 1, \\ \psi_i(x^\pm, \sigma, \tau) e^{\mp s_-(x, \sigma, \tau)} = O(1), & \text{as } x \rightarrow -1, \end{cases} \end{aligned}$$

where  $s_\pm(x, \sigma, \tau) = \frac{i\kappa}{2} \frac{\tau \pm \sigma}{1 \mp x}$  is obtained from the Virasoro constraints. Thus the line bundle  $L_{\sigma, \tau} \rightarrow \Sigma$  uniquely specifies an equivalence class of divisors  $[\hat{\gamma}]$  of degree  $\deg \hat{\gamma} = g + 1$ . In fact one can show [15], taking particular care of the global  $SU(2)_R$  degrees of freedom of the string, that this construction leads to an injective map

$$j \mapsto \{\Sigma, dp, \hat{\gamma}\}, \tag{1.3}$$

where the differential  $dp$  on  $\Sigma$  is such that the pair  $(\Sigma, dp)$  encodes all the moduli of the spectral curve  $\Gamma$ . The reconstruction of finite-gap solutions can now be achieved by constructing the left-inverse of the injective map (1.3). This is done with the help of special functions on the Riemann surface  $\Sigma$  known as Riemann  $\theta$ -functions. The reconstruction of

the sigma-model field  $g \in SU(2)$ , out of which  $j = -g^{-1}dg$  is built, requires the concept of the dual Baker-Akhiezer vector  $\boldsymbol{\psi}^+$ . It is constructed in such a way that it obeys the following orthogonality relation with the Baker-Akhiezer vector

$$\boldsymbol{\psi}^+(P) \cdot \boldsymbol{\psi}(P) = 1, \quad \boldsymbol{\psi}^+(\hat{\sigma}P) \cdot \boldsymbol{\psi}(P) = 0. \quad (1.4)$$

Explicitly its components are given as follows

$$\psi_1^+(P) = \chi(P)\tilde{\psi}_1^+(P), \quad \psi_2^+(P) = \frac{\chi(P)}{\chi(\infty^-)}\tilde{\psi}_2^+(P),$$

where  $\chi(P)$  is meromorphic on  $\Sigma$  with divisor  $(\chi) = \hat{\gamma} \cdot \hat{\tau}\hat{\gamma} \cdot B^{-1}$  ( $B$  being the divisor of branch points of  $\Sigma$ ) and normalised by  $\chi(\infty^+) = 1$ , and  $\tilde{\boldsymbol{\psi}}^+(P)$  is a Baker-Akhiezer vector on  $\Sigma$  relative to the data  $\{\hat{\tau}\hat{\gamma}, -s_{\pm}\}$ , which therefore satisfies the reality condition

$$\boldsymbol{\psi}(\hat{\tau}P)^\dagger = \tilde{\boldsymbol{\psi}}^+(P). \quad (1.5)$$

It follows using both (1.4) and (1.5) that when  $\hat{\tau}P = P$  (or equivalently when  $\hat{\pi}(P) \in \mathbb{R}$ ) one has

$$\psi_1(\hat{\sigma}P) = -\frac{A(P)}{\chi(\infty^-)}\overline{\psi_2(P)}, \quad \psi_2(\hat{\sigma}P) = A(P)\overline{\psi_1(P)},$$

where  $A(P) \equiv \chi(P) \det(\boldsymbol{\psi}(P), \boldsymbol{\psi}(\hat{\sigma}P))$ . Now by definition of  $j = -g^{-1}dg$ , the matrix  $g^{-1} \in SL(2, \mathbb{C})$  satisfies  $dg^{-1} = jg^{-1}$  and hence since  $j = J(0)$  we have

$$g^{-1} = \frac{1}{\sqrt{\det \Psi(0)}} \Psi(0),$$

up to an  $SL(2, \mathbb{C})$  transformation  $g \mapsto \tilde{g}_L \cdot g$  and where

$$\begin{aligned} \Psi(0) &= (\boldsymbol{\psi}(0^+), \boldsymbol{\psi}(0^-)) = \begin{pmatrix} \psi_1(0^+) & \psi_1(0^-) \\ \psi_2(0^+) & \psi_2(0^-) \end{pmatrix}, \\ &= \begin{pmatrix} \psi_1(0^+) & -\frac{1}{\chi(\infty^-)}\overline{\psi_2(0^+)} \\ \psi_2(0^+) & \psi_1(0^+) \end{pmatrix} \text{diag}(1, A(0^+)), \\ &= \tilde{g}_R \begin{pmatrix} \psi_1(0^+) & -\chi(\infty^-)^{-\frac{1}{2}}\overline{\psi_2(0^+)} \\ \chi(\infty^-)^{-\frac{1}{2}}\psi_2(0^+) & \psi_1(0^+) \end{pmatrix} \tilde{g}_L, \end{aligned}$$

with  $\tilde{g}_R = \text{diag}(1, \chi(\infty^-)^{\frac{1}{2}})$  and  $\tilde{g}_L = \text{diag}(1, \chi(\infty^-)^{-\frac{1}{2}}A(0^+))$ . Thus finally, after a residual  $SL(2, \mathbb{C})_R \times SL(2, \mathbb{C})_L$  transformation (c.f. [14] p43) the reconstructed matrix  $g^{-1}$  lives in  $SU(2)$ ,

$$g = \begin{pmatrix} Z_1 & Z_2 \\ -\bar{Z}_2 & \bar{Z}_1 \end{pmatrix}, \quad (1.6)$$

where

$$Z_1 = C\tilde{\psi}_1^+(0^+), \quad Z_2 = \frac{C}{\chi(\infty^-)^{\frac{1}{2}}}\tilde{\psi}_2^+(0^+) \quad (1.7)$$

and  $C \in \mathbb{R}$  is a normalisation constant chosen such that  $|Z_1|^2 + |Z_2|^2 = 1$ .

It is clear from the above construction that the (dual) Baker-Akhiezer vector does not depend on the choice of canonical homology basis for  $H_1(\Sigma, \mathbb{Z})$  and so neither does the general finite-gap solution (1.7). However, when explicitly constructing the solution in terms of  $\theta$ -functions on  $\Sigma$  as we will do below a particular choice of canonical homology basis for  $H_1(\Sigma, \mathbb{Z})$  is required. Different choices of  $a$ - and  $b$ -cycles, connected to one another by an  $\text{Sp}(2g, \mathbb{Z})$  transformation, offer alternative but equivalent parametrisations of one and the same finite-gap solution. Furthermore, one is also free to make a different choice of branch cuts when representing the Riemann surface  $\Sigma$  as a two-sheeted ramified cover of  $\mathbb{CP}^1$  since the cuts are not an intrinsic property of  $\Sigma$ . These remarks will be essential later when we come to study the Hofman-Maldacena limit of the finite-gap solutions.

The Baker-Akhiezer vector  $\tilde{\psi}^+$  can be reconstructed explicitly using Riemann  $\theta$ -functions, in particular we find for the components of  $\tilde{\psi}^+(0^+)$

$$\tilde{\psi}_1^+(0^+) = h_-(0^+) \frac{\theta(\mathbf{D}; \Pi) \theta(2\pi \int_{\infty^+}^{0^+} \boldsymbol{\omega} - \int_{\mathbf{b}} d\mathcal{Q} - \mathbf{D}; \Pi)}{\theta(\int_{\mathbf{b}} d\mathcal{Q} + \mathbf{D}; \Pi) \theta(2\pi \int_{\infty^+}^{0^+} \boldsymbol{\omega} - \mathbf{D}; \Pi)} \exp \left( +\frac{i}{2} \int_{\infty^-}^{\infty^+} d\mathcal{Q} - \frac{i}{2} \int_{0^-}^{0^+} d\mathcal{Q} \right), \quad (1.8a)$$

$$\tilde{\psi}_2^+(0^+) = h_+(0^+) \frac{\theta(\mathbf{D}; \Pi) \theta(2\pi \int_{\infty^-}^{0^+} \boldsymbol{\omega} - \int_{\mathbf{b}} d\mathcal{Q} - \mathbf{D}; \Pi)}{\theta(\int_{\mathbf{b}} d\mathcal{Q} + \mathbf{D}; \Pi) \theta(2\pi \int_{\infty^-}^{0^+} \boldsymbol{\omega} - \mathbf{D}; \Pi)} \exp \left( -\frac{i}{2} \int_{\infty^-}^{\infty^+} d\mathcal{Q} - \frac{i}{2} \int_{0^-}^{0^+} d\mathcal{Q} \right). \quad (1.8b)$$

Here  $h_{\pm}(P)$  are meromorphic functions on  $\Sigma$  defined as follows

$$(h_{\pm}) \geq \infty^{\pm} (\hat{\gamma}^+)^{-1}, \quad h_{\pm}(\infty^{\mp}) = 1,$$

and the vector  $\mathbf{D} \equiv \mathcal{A}(\hat{\gamma}^+) - \mathcal{A}(\infty^-) + \mathcal{K} \in \mathbb{C}^g$  is almost<sup>1</sup> arbitrary, where  $\mathcal{A}(P) = 2\pi \int_{\infty^+}^P \boldsymbol{\omega}$  is the Abel map<sup>2</sup> and  $\mathcal{K}$  is the vector of Riemann constants which can be related in a simple way to the canonical class  $Z$  (the divisor class of any meromorphic differential), namely [23]

$$2\mathcal{K} = -\mathcal{A}(Z). \quad (1.9)$$

The components  $\{\omega_i\}_{i=1}^g$  of the vector  $\boldsymbol{\omega}$  are the basis holomorphic differentials on  $\Sigma$  defined by their  $a$ -periods

$$\int_{a_i} \omega_j = \delta_{ij},$$

---

<sup>1</sup>‘almost’ refers to the fact that  $\theta(\mathcal{A}(P) - \mathbf{D})$  shouldn’t vanish identically.

<sup>2</sup>The integration contour from  $\infty^+$  to  $P$  in  $\mathcal{A}(P) = 2\pi \int_{\infty^+}^P \boldsymbol{\omega}$  is taken to lie within the normal form  $\Sigma_{\text{cut}}$  of  $\Sigma$  defined by cutting the Riemann surface  $\Sigma$  along the cycles  $a, b$ . This corresponds to a choice of branch for the multi-valued Abelian integral  $\int^P \boldsymbol{\omega}$ .

and in terms of which the period matrix  $\Pi$  can be defined

$$\Pi_{ij} = \int_{b_i} \omega_j.$$

A special role is played in the formulae (1.8) by the differential  $d\mathcal{Q} = \frac{1}{2\pi}(\sigma dp + \tau dq)$  where  $dp, dq$  are the normalised<sup>3</sup> differentials of the quasi-momentum and quasi-energy. Finally,

$$\theta(\mathbf{z}; \Pi) \equiv \sum_{\mathbf{m} \in \mathbb{Z}^g} \exp \{i \langle \mathbf{m}, \mathbf{z} \rangle + \pi i \langle \Pi \mathbf{m}, \mathbf{m} \rangle\}, \quad \text{for } \mathbf{z} \in \mathbb{C}^g \quad (1.10)$$

is the Riemann  $\theta$ -function associated with the Riemann surface  $\Sigma$ .

By uniqueness of the (dual) Baker-Akhiezer vector the reconstruction formulae (1.8) give the same solution for any choice of basis of  $H_1(\Sigma, \mathbb{Z})$ , but the reality conditions on the various ingredients in (1.8) are dependent on this choice of basis. This is because we may choose a basis for which the  $a$ -cycles say are imaginary  $\hat{\tau}a_i = -a_i$  and the  $b$ -cycles are real  $\hat{\tau}b_i = b_i$ , but we may just as well choose a basis for which the reverse is true,  $\hat{\tau}a_i = a_i$  and  $\hat{\tau}b_i = -b_i$ . This does not mean that the solution exhibits different reality properties for different choices of  $a$ - and  $b$ -cycles, but only that the parameters of the solution may have different reality properties for different choices of cycles; the resulting matrix  $g$  in (1.6) is always  $SU(2)$  valued. Equation (1.9) allows us to reformulate the reality conditions on  $\mathcal{A}(\hat{\gamma}^+)$  obtained in [14] (with respect to the canonical homology basis of that paper), as reality conditions on the vector  $\mathbf{D}$  since

$$\begin{aligned} 2\text{Im } \mathcal{A}(\hat{\gamma}^+) &= \mathcal{A}(Z \cdot (\infty^-)^2 \cdot (\infty^+)^2) \\ &= \mathcal{A}(Z) + 2\mathcal{A}(\infty^-) \\ &= 2\mathcal{A}(\infty^-) - 2\mathcal{K}, \\ \Rightarrow \quad \text{Im } \mathbf{D} &= 0, \end{aligned} \quad (1.11)$$

where we have used the fact that  $\overline{\mathcal{K}} = -\mathcal{K}$  and  $\overline{\mathcal{A}(\infty^-)} = -\mathcal{A}(\infty^-)$  hold as equalities on the Jacobian  $J(\Sigma)$ , which themselves follow from  $\overline{\hat{\tau}^* \omega} = -\omega$ .

Let us also specify an alternative definition to (1.9) of the vector of Riemann constants  $\mathcal{K}$  which will come in handy later. One can show with our conventions that the components of  $\mathcal{K}$  are given by the following formulae

$$\mathcal{K}_k = 2\pi \left[ \frac{1 + \Pi_{kk}}{2} - \sum_{j=1, j \neq k}^g \int_{a_j} \left( \int_{\infty^+}^P \omega_k \right) \omega_j \right]. \quad (1.12)$$

---

<sup>3</sup>An Abelian differential  $\Omega$  of the second or third kind is said to be *normalised* if its  $a$ -periods are all set to zero,  $\int_{a_i} \Omega = 0, i = 1, \dots, g$ .



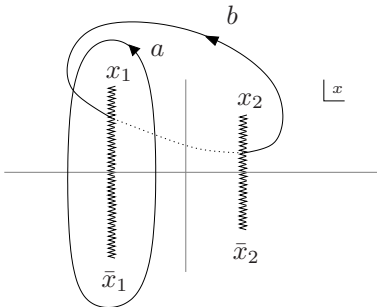


Figure 1:  $a$ - and  $b$ -periods in  $x$ -plane.

## 2 Elliptic (two-gap) case

When the underlying curve  $\Sigma$  of the previous section is elliptic (genus 1), everything within the expressions (1.7), (1.8) for the general finite-gap solution can be explicitly computed in terms of elliptic functions. The aim of this section is to obtain the most general elliptic finite-gap solution. To avoid cluttering this section with lengthy calculations we shall refer to a series of appendices for the details.

So consider the most general (real<sup>4</sup>) elliptic curve given algebraically by

$$y^2 = (x - x_1)(x - \bar{x}_1)(x - x_2)(x - \bar{x}_2), \quad (2.1)$$

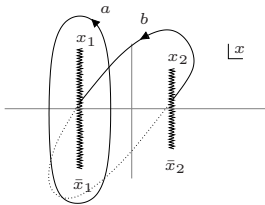
which can be represented as a 2-sheeted Riemann surface with 2 cuts. The  $a$ - and  $b$ -periods of the curve are chosen<sup>5</sup> as in Figure 1. On this curve we can define a unique normalised (vanishing  $a$ -period) holomorphic differential

$$\omega = \nu / \int_a \nu,$$

---

<sup>4</sup>The reality condition on the curve must be imposed, which simply requires the set of branch points  $\{x_1, x_2, \bar{x}_1, \bar{x}_2\}$  to be invariant under conjugation  $x \mapsto \bar{x}$ , see [14] for details.

<sup>5</sup>Note that for the  $b$ -period we are using a slightly different convention to that in [14]. In [14] the  $b$ -period would join  $x_2$  to  $\bar{x}_1$



This change of convention is convenient in the elliptic case under consideration here because in this case (and only this case) the period matrix  $\Pi$  (which is a single complex number  $\tau$  in this case) turns out to be purely imaginary.

where  $\nu = dx/y$  is a holomorphic differential on (2.1). The period matrix in the elliptic case is just a single complex number which we compute in appendix A to be,

$$\Pi = \int_b \omega = \int_b \nu / \int_a \nu = \frac{iK'}{K} \equiv \tau,$$

where  $K(k)$  and  $K'(k) = K(k')$  are the elliptic integrals of the first kind depending on the elliptic modulus  $k$  of the curve and its dual modulus  $k'$  defined as,

$$k' = \left| \frac{x_1 - x_2}{x_1 - \bar{x}_2} \right|, \quad k = \sqrt{1 - (k')^2}.$$

The Riemann  $\theta$ -function reduces in the elliptic case to the Jacobi  $\vartheta$ -function

$$\vartheta_3(z; \tau) = \sum_{n=-\infty}^{\infty} \exp(\pi i n^2 \tau + 2\pi i n z) = \theta(2\pi z; \tau).$$

It is useful to define three other Jacobi  $\vartheta$ -functions as translations of  $\vartheta_3(z; \tau)$  by half-periods, namely

$$\begin{aligned} \vartheta_0(z; \tau) &= \vartheta_3\left(z + \frac{1}{2}; \tau\right), \\ \vartheta_1(z; \tau) &= \exp\left(\pi i \frac{\tau}{4} + \pi i \left(z + \frac{1}{2}\right)\right) \vartheta_3\left(z + \frac{\tau+1}{2}; \tau\right), \\ \vartheta_2(z; \tau) &= \exp\left(\pi i \frac{\tau}{4} + \pi i z\right) \vartheta_3\left(z + \frac{\tau}{2}; \tau\right). \end{aligned}$$

We also introduce the Jacobi  $\Theta$ -functions which depend directly on the elliptic modulus  $k$  of the elliptic curve

$$\Theta_\mu(z; k) \equiv \vartheta_\mu\left(\frac{z}{2K}; \tau = \frac{iK'}{K}\right), \quad \mu = 0, \dots, 3.$$

When there is no ambiguity as to what the elliptic modulus  $k$  is we will omit it from the arguments and simply write  $\Theta_\mu(z) = \Theta_\mu(z; k)$ .

In appendix B we compute explicitly in the elliptic case the various ingredients appearing inside the  $\theta$ -functions of (1.8). We show for instance that the real parts of  $\int_{\infty^\pm}^{0^+} \omega$  are  $\frac{1}{2}$  and 0 respectively so that we can write

$$\int_{\infty^+}^{0^+} \omega = \frac{1}{2} + i\rho_+, \quad \int_{\infty^-}^{0^+} \omega = \frac{\tau}{2} + i\rho_-. \quad (2.2)$$

Here  $\rho_\pm \in \mathbb{R}$  are real numbers function of the moduli of the elliptic curve. The reason for the shift by  $\frac{\tau}{2}$  in the second of these integrals (which could be absorbed into the arbitrary

constant  $\rho_-$ ) will become clear later. At this stage we can already simplify the reconstruction formulae (1.7) a bit

$$Z_1 = Ch_-(0^+) \frac{\vartheta_0(X_0; \tau) \vartheta_3(X - i\rho_+; \tau)}{\vartheta_3(X_0 - i\rho_+; \tau) \vartheta_0(X; \tau)} \exp \left( -i \int_{\infty^+}^{0^+} d\mathcal{Q} \right), \quad (2.3a)$$

$$Z_2 = C \frac{h_+(0^+)}{\chi(\infty^-)^{\frac{1}{2}}} \frac{\vartheta_0(X_0; \tau) \vartheta_1(X - i\rho_-; \tau)}{\vartheta_1(X_0 - i\rho_-; \tau) \vartheta_0(X; \tau)} \exp \left( -i \int_{\infty^-}^{0^+} d\mathcal{Q} + \frac{i}{2} \int_b d\mathcal{Q} \right), \quad (2.3b)$$

where we have defined  $X \equiv \frac{1}{2\pi} \int_b d\mathcal{Q} + X_0$  and  $X_0 \equiv \frac{1}{2\pi} D - \frac{1}{2} \in \mathbb{R}$ , or if we define the notation  $\tilde{A} = 2KA$  then

$$Z_1 = Ch_-(0^+) \frac{\Theta_0(\tilde{X}_0) \Theta_3(\tilde{X} - i\tilde{\rho}_+)}{\Theta_3(\tilde{X}_0 - i\tilde{\rho}_+) \Theta_0(\tilde{X})} \exp \left( -i \int_{\infty^+}^{0^+} d\mathcal{Q} \right), \quad (2.4a)$$

$$Z_2 = C \frac{h_+(0^+)}{\chi(\infty^-)^{\frac{1}{2}}} \frac{\Theta_0(\tilde{X}_0) \Theta_1(\tilde{X} - i\tilde{\rho}_-)}{\Theta_1(\tilde{X}_0 - i\tilde{\rho}_-) \Theta_0(\tilde{X})} \exp \left( -i \int_{\infty^-}^{0^+} d\mathcal{Q} + \frac{i}{2} \int_b d\mathcal{Q} \right). \quad (2.4b)$$

Expressions for the variables  $\rho_{\pm}$  in terms of the moduli of the curve can also be obtained. In appendix B we derive a closed form expression for the integrals in (2.2), namely

$$\int_{\infty^{\pm}}^{0^+} \omega = \frac{iF(\varphi_{\mp}, k')}{2K}, \quad (2.5)$$

where,

$$\tan \frac{\varphi_{\pm}}{2} = \frac{(\sqrt{\bar{x}_2} \pm \sqrt{\bar{x}_1})(\sqrt{\bar{x}_1} + \sqrt{\bar{x}_2})}{|x_1 - \bar{x}_2|}. \quad (2.6)$$

From these equations we conclude that the real variables  $\rho_{\pm}$  depend not only on the magnitude  $k' = |h|$  of  $h$  but also on another real parameter, related to the phase of  $h$ . This is just what we require to exhibit the fact that  $\rho_{\pm}$  do contain a free parameter of the solution. However, because we are dealing with a 2-cut finite-gap solution there cannot be more than 3 independent conserved quantities [14, 15]: the two global charges  $R$  and  $L$  or equivalently  $J_1 = (L - R)/2$  and  $J_2 = (L + R)/2$ , and the single internal charge (recall [14, 15] that in the general case with genus  $g$  there are  $g$  internal charges).

Gathering together equations (2.2) and (2.5) we have  $i\tilde{\rho}_- + iK' = iF(\varphi_+, k')$  from which one can deduce that

$$i\rho_- = 0 \Leftrightarrow \tan \frac{\varphi_+}{2} = 1 \Leftrightarrow \arg \left( \frac{x_1}{\bar{x}_2} \right) \in \pi\mathbb{Z}.$$

An example which meets this condition is when the set of branch points  $\{x_1, x_2, \bar{x}_1, \bar{x}_2\}$  of the curve has the extra symmetry  $x \rightarrow -x$ . However, with  $\bar{x}_2 = -x_1$  we find  $\tan \frac{\varphi_-}{2} = -i$ .

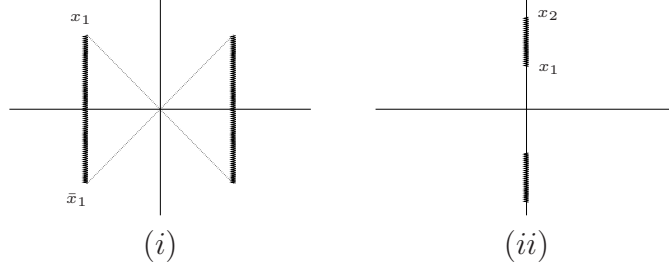


Figure 2: two distinct possible limits of elliptic finite-gap solutions under Frolov-Tseytlin limit  $\rho_{\pm} \rightarrow 0$ .

Then, putting together the equations (2.2) and (2.5) we have  $K + i\tilde{\rho}_+ = iF(\varphi_-, k')$ , which yields

$$\rho_+ = 0.$$

It is clear then that the Frolov-Tseytlin solution (for which the curve has the extra symmetry  $x \rightarrow -x$ ) corresponds to the case  $\rho_{\pm} = 0$ . In this limit the space of solutions breaks up into two distinct non-singular sectors:

- (i)  $x_1 = -\bar{x}_2$ , in which case the curve  $\Sigma$  is parametrised by a single complex number  $x_1 \in \mathbb{C}$ , and corresponds to the “double contour” configuration of Bethe roots on the gauge theory side (see Figure 2 (i)).
- (ii)  $x_1 = -\bar{x}_1, x_2 = -\bar{x}_2$ , in which case the curve  $\Sigma$  is parametrised by two real numbers  $ix_1, ix_2 \in \mathbb{R}$ , and corresponds to the “imaginary root” configuration of Bethe roots (see Figure 2 (ii)).

To go from one sector to the other without violating the reality condition or the symmetry  $x \rightarrow -x$  one has to go through the common singular limit  $k \rightarrow 1$  of both sectors. So the two sectors (i), (ii) are effectively disconnected regions of the parameter space for non-singular  $\Sigma$  in the Frolov-Tseytlin limit  $\rho_{\pm} \rightarrow 0$ .

Next we obtain the  $b$ -periods for the differential  $d\mathcal{Q}$ . Using the Riemann bilinear identities for the differentials  $dp$  and  $\omega$  one finds

$$\int_b dp = -2\pi i \sum \text{res } p\omega,$$

where the Abelian integral  $p(P) = \int^P dp$  has simple poles at  $x = \pm 1$  of the form<sup>6</sup>

$$p(x) \sim \frac{\pi\kappa}{x \mp 1} \quad \text{as } x \rightarrow \pm 1. \quad (2.7)$$

---

<sup>6</sup>In [14, 15] the overall sign was different and we had  $p(x) \underset{x \rightarrow \pm 1}{\sim} -\frac{\pi\kappa}{x \mp 1}$ . However, this difference of sign simply comes down to the choice of the physical sheet.

And so, using expression (A.8) for the holomorphic differential  $\omega$  we obtain

$$\frac{1}{2\pi} \int_b dp = \frac{\pi\kappa|x_1 - \bar{x}_2|}{2K} \left( \frac{1}{y_+} + \frac{1}{y_-} \right), \quad (2.8)$$

where  $y_{\pm} = y(x)|_{x=\pm 1} > 0$  by the choice of branch for the function  $y$  (see appendix A). Likewise, for the Abelian integral  $q(P) = \int^P dq$  whose simple poles at  $x = \pm 1$  are of the form

$$q(x) \sim \pm \frac{\pi\kappa}{x \mp 1} \quad \text{as } x \rightarrow \pm 1, \quad (2.9)$$

one obtains

$$\frac{1}{2\pi} \int_b dq = \frac{\pi\kappa|x_1 - \bar{x}_2|}{2K} \left( \frac{1}{y_+} - \frac{1}{y_-} \right). \quad (2.10)$$

Now equations (2.8) and (2.10) together imply

$$\left( \frac{1}{2\pi} \int_b dp \right)^2 - \left( \frac{1}{2\pi} \int_b dq \right)^2 = \frac{\pi^2 \kappa^2 |x_1 - \bar{x}_2|^2}{K^2 y_+ y_-},$$

so that if we define rescaled coordinates

$$(x, t) = (\kappa' \sigma, \kappa' \tau) \quad \text{where} \quad \kappa' \equiv \kappa \frac{|x_1 - \bar{x}_2|}{\sqrt{y_+ y_-}},$$

then

$$\begin{aligned} X - X_0 &= \frac{1}{2\pi} \int_b d\mathcal{Q} = \left( \frac{1}{4\pi^2} \int_b dp \right) \sigma + \left( \frac{1}{4\pi^2} \int_b dq \right) \tau, \\ &= \frac{1}{2} \left( \sqrt{\frac{y_-}{y_+}} + \sqrt{\frac{y_+}{y_-}} \right) \frac{x}{2K} + \frac{1}{2} \left( \sqrt{\frac{y_-}{y_+}} - \sqrt{\frac{y_+}{y_-}} \right) \frac{t}{2K}, \\ &= \frac{1}{2K} \frac{x - vt}{\sqrt{1 - v^2}}, \end{aligned}$$

where

$$v \equiv \frac{y_+ - y_-}{y_+ + y_-}.$$

Note that  $|v| < 1$  since  $y_{\pm} > 0$ . So the scaled variable  $\tilde{X}$  appearing in (2.4) satisfies

$$\tilde{X} = \tilde{X}_0 + \frac{x - vt}{\sqrt{1 - v^2}}.$$

Let us also define a boosted time coordinate

$$\tilde{T} = \frac{1}{2} \left( \sqrt{\frac{y_-}{y_+}} + \sqrt{\frac{y_+}{y_-}} \right) t + \frac{1}{2} \left( \sqrt{\frac{y_-}{y_+}} - \sqrt{\frac{y_+}{y_-}} \right) x = \frac{t - vx}{\sqrt{1 - v^2}}.$$

In appendix C we express the exponents in (1.8) in terms of elliptic integrals. The details of this computation are not important and so we simply state the result here. The general elliptic finite-gap solutions (2.4) now takes the following form

$$Z_1 = Ch_-(0^+) \frac{\Theta_0(\tilde{X}_0)\Theta_3(\tilde{X} - i\tilde{\rho}_+)}{\Theta_3(\tilde{X}_0 - i\tilde{\rho}_+)\Theta_0(\tilde{X})} \exp\left(Z_2(i\tilde{\rho}_+, k) (\tilde{X} - \tilde{X}_0) + iv_+\tilde{T}\right), \quad (2.11a)$$

$$Z_2 = C \frac{h_+(0^+)}{\chi(\infty^-)^{\frac{1}{2}}} \frac{\Theta_0(\tilde{X}_0)\Theta_1(\tilde{X} - i\tilde{\rho}_-)}{\Theta_1(\tilde{X}_0 - i\tilde{\rho}_-)\Theta_0(\tilde{X})} \exp\left(Z_0(i\tilde{\rho}_-, k) (\tilde{X} - \tilde{X}_0) + iv_-\tilde{T}\right), \quad (2.11b)$$

where we have defined

$$v_{\pm} = \frac{y(0) \pm 1}{|x_1 - \bar{x}_2|},$$

which satisfy  $v_-^2 - v_+^2 = \text{dn}^2(i\tilde{\rho}_-, k) + (k')^2 \text{sc}^2(i\tilde{\rho}_+, k)$ .

Finally, all that remains to be determined are the normalisation constants in (2.11) which are obtained in appendix D,

$$\begin{aligned} h_-(0^+) &= \frac{\vartheta_3(X_0 - i\rho_+)}{\vartheta_2(i\rho_+)} = \frac{\Theta_3(\tilde{X}_0 - i\tilde{\rho}_+)}{\Theta_2(i\tilde{\rho}_+)}, \\ \frac{h_+(0^+)}{\chi(\infty^-)^{\frac{1}{2}}} &= \frac{\vartheta_1(X_0 - i\rho_-)}{\vartheta_0(i\rho_-)} = \frac{\Theta_1(\tilde{X}_0 - i\tilde{\rho}_-)}{\Theta_0(i\tilde{\rho}_-)}. \end{aligned} \quad (2.12)$$

Plugging these constants back into the general elliptic finite-gap solutions (2.11) yields

$$Z_1 = C \frac{\Theta_3(\tilde{X} - i\tilde{\rho}_+)}{\Theta_2(i\tilde{\rho}_+)\Theta_0(\tilde{X})} \exp\left(Z_2(i\tilde{\rho}_+, k)\tilde{X} + iv_+\tilde{T} + i\varphi_1^0\right), \quad (2.13a)$$

$$Z_2 = C \frac{\Theta_1(\tilde{X} - i\tilde{\rho}_-)}{\Theta_0(i\tilde{\rho}_-)\Theta_0(\tilde{X})} \exp\left(Z_0(i\tilde{\rho}_-, k)\tilde{X} + iv_-\tilde{T} + i\varphi_2^0\right), \quad (2.13b)$$

where we have introduced global phases  $\varphi_i^0, i = 1, 2$  into which we have absorbed the terms in the exponentials involving  $\tilde{X}_0$ . Notice that this solution corresponds exactly (up to a trivial interchange of coordinates  $Z_1 \leftrightarrow Z_2$ ) to the type (i) helical string with two spins of [16] when  $X_0 = \varphi_1^0 = \varphi_2^0 = 0$ . However (2.13) does contain the extra ‘initial value’ degree of freedom compared to the type (i) helical string which corresponds to the initial value of the internal degree of freedom. The initial values  $\varphi_i^0, i = 1, 2$  of the global  $SU(2)_R \times SU(2)_L$  degrees of freedom have also been trivially included.

## 2.1 Global charges

In this section we discuss the global conserved charges  $L, R$  corresponding to the Casimirs of the global  $SU(2)_R \times SU(2)_L$  symmetry as well as the space-time energy  $E$  of the string corresponding to translation invariance in the target time coordinate  $X_0$ . The moduli of the elliptic curve  $\Sigma$  which encodes the conserved quantities of the solution can be succinctly described in terms of a special differential [14]

$$\alpha \equiv \frac{\sqrt{\lambda}}{4\pi} \left( x + \frac{1}{x} \right) dp, \quad (2.14)$$

where  $dp$  is the quasi-momentum invoked previously. In particular, the global charges  $L, R$  are both expressed in terms of the residues of  $\alpha$  at  $0^+, \infty^+$  respectively<sup>7</sup>,

$$\frac{L}{2} = -\text{res}_{0^+} \alpha, \quad \frac{R}{2} = \text{res}_{\infty^+} \alpha. \quad (2.15)$$

Let us define from  $L, R$  the usual linear combinations  $J_1, J_2$  of conserved charges that are relevant for comparison with the gauge theory, namely

$$\begin{aligned} J_1 &= \frac{L + R}{2} = -\text{res}_{0^+} \alpha + \text{res}_{\infty^+} \alpha, \\ J_2 &= \frac{L - R}{2} = -\text{res}_{0^+} \alpha - \text{res}_{\infty^+} \alpha. \end{aligned} \quad (2.16)$$

In section 3.1 we will want to consider the Hofman-Maldacena limits of these charges. In this limit we will see that the two cuts of the elliptic curve merge together to leave behind a pair of complex conjugate singular points in the  $x$ -plane. Thus it will be useful to consider the situation where  $x = 0$  lies outside the region in between the two cuts. The charge  $J_2$  can be broken down into a sum of contributions from each pair of branch points of  $\Sigma$  for we have

$$J_2 = \frac{1}{2\pi i} \int_{a_1} \alpha + \frac{1}{2\pi i} \int_{a_2} \alpha = \frac{1}{2\pi i} \int_{b_1} \alpha + \frac{1}{2\pi i} \int_{b_2} \alpha = 2\text{Re} \left[ \frac{1}{2\pi i} \int_{b_1} \alpha \right], \quad (2.17)$$

where the cycles  $a_i, b_i, i = 1, 2$  are depicted in Figure 3. The total space-time energy  $E$  of the string which has a simple form in static gauge  $X_0 = \kappa\tau$ ,

$$E \equiv \frac{\sqrt{\lambda}}{2\pi} \int_0^{2\pi} d\sigma \partial_\tau X_0 = \kappa\sqrt{\lambda}. \quad (2.18)$$

To obtain a similar expression to (2.17) but for the other charge  $J_2$  we consider the differential

$$\tilde{\alpha} \equiv \frac{\sqrt{\lambda}}{4\pi} \left( x - \frac{1}{x} \right) dp = \frac{\sqrt{\lambda}}{4\pi} \frac{(x-1)(x+1)}{x} dp. \quad (2.19)$$

---

<sup>7</sup>The overall sign here is different from that in [14, 15] for the same reason that the sign in (2.7) was different.

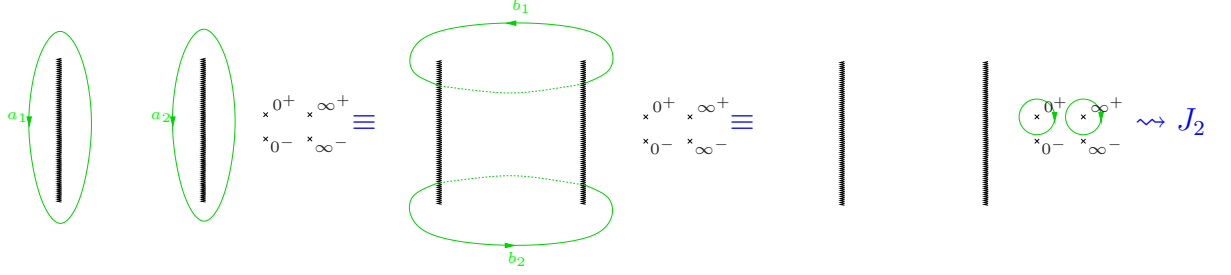


Figure 3: Contributions to global charge  $J_2$  from pairs of branch points.

It has simple poles at  $x = \pm 1$ ,  $x = 0$  and  $x = \infty$  on the top sheet by virtue of the fact that  $dp$  has only double poles at  $x = \pm 1$  of the form

$$dp(x) = d\left(\frac{\pi\kappa}{x \mp 1}\right) + O((x \mp 1)^0), \quad \text{as } x \rightarrow \pm 1.$$

Thus we can write

$$0 = \sum_{I=1}^2 \frac{1}{2\pi i} \int_{a_I} \tilde{\alpha} + \sum_{x \in \{\pm 1, 0, \infty\}} \text{res}_x \tilde{\alpha},$$

which can be simplified using (2.19), the definitions of  $E$  and  $J_1$ , and the fact that the sum of the  $a_I$ -periods of  $\tilde{\alpha}$  is equal to the sum of its  $b_I$ -periods, yielding

$$E - J_1 = \sum_{I=1}^2 \frac{1}{2\pi i} \int_{b_I} \tilde{\alpha} = 2\text{Re} \left[ \frac{1}{2\pi i} \int_{b_1} \tilde{\alpha} \right]. \quad (2.20)$$

This is to be compared with the expression for  $J_2$  in (2.17).

## 2.2 Periodicity

All finite-gap solutions are quasi-periodic since the dynamical divisor  $\hat{\gamma}(x, t)$  moves linearly

$$\mathcal{A}(\hat{\gamma}(x, t)) = \mathcal{A}(\hat{\gamma}(x_0, t_0)) + \left( \frac{1}{2\pi} \int_b dp \right) \frac{x - x_0}{\kappa'} + \left( \frac{1}{2\pi} \int_b dq \right) \frac{t - t_0}{\kappa'} \in J(\Sigma), \quad (2.21)$$

on the Jacobian  $J(\Sigma)$  which is a compact complex torus [14]. Since the string is closed we require the two-cut solution (2.13) to be real  $\sigma$ -periodic and so we must impose the condition

$$\frac{1}{2\pi} \int_b dp \equiv n \in \mathbb{Z}. \quad (2.22)$$

Equation (2.8) then implies

$$\frac{\pi\kappa|x_1 - \bar{x}_2|}{2K} \left( \frac{1}{y_+} + \frac{1}{y_-} \right) = n,$$



which can equivalently be rewritten as

$$\frac{2K\sqrt{1-v^2}}{\kappa'} = \frac{2\pi}{n}. \quad (2.23)$$

It is clear from the periodicity property  $\Theta_\mu(z+2K) = \Theta_\mu(z)$  of  $\Theta$ -functions that the fundamental period in the  $x$  variable of the  $\Theta$ -function part of the formula (2.13) is

$$T_x \equiv 2K\sqrt{1-v^2} = \frac{2\pi\kappa'}{n}. \quad (2.24)$$

Thus we can break up the full closed string interval  $x \in [-\pi\kappa', \pi\kappa']$  (i.e.  $\sigma \in [-\pi, \pi]$ ) into  $n$  equal intervals, referred to as ‘hops’ in [16], corresponding to regions of periodicity of the internal degrees of freedom. In the next section we shall restrict attention to the following ‘single-hop’ region

$$-\frac{1}{2}T_x \leq x < \frac{1}{2}T_x. \quad (2.25)$$

A ‘single-hop’ corresponds in the algebro-geometric language to a single traverse of the Jacobian  $J(\Sigma)$  by the dynamical divisor  $\hat{\gamma}(x, t)$  as is clear from (2.21), or put another way, a single traverse of a homology  $a$ -cycle by the divisor  $\hat{\gamma}(x, t)$  on  $\Sigma$ .

Besides the condition (2.22) which comes from periodicity requirements on the internal degrees of freedom, another periodicity condition comes from considering the global  $SU(2)_R \times SU(2)_L$  degrees of freedom in the exponentials of (2.13), leading to

$$\frac{1}{2\pi} \int_{\infty^\pm}^{0^+} dp \equiv -N_\pm \in \mathbb{Z}. \quad (2.26)$$

This is the statement that after a full traverse of the string interval  $\sigma \in [0, 2\pi]$  the arguments of the exponentials should have changed by integer multiples of  $2\pi$ . Restricting attention to the ‘single-hop’ region we must require that the arguments of the exponentials only change by integer multiples of  $\frac{2\pi}{n}$ . In other words, combining (2.26) with equations (C.6) and (C.7) yields the final periodicity conditions

$$\begin{aligned} 2K [-iZ_0(i\tilde{\rho}_-, k) - v \cdot v_-] - \pi &= \frac{2\pi N_-}{n}, \\ 2K [-iZ_2(i\tilde{\rho}_+, k) - v \cdot v_+] &= \frac{2\pi N_+}{n}, \end{aligned} \quad (2.27)$$

which correspond to the changes in the exponentials over a ‘single-hop’.

## 3 Singular curve

### 3.1 Giant magnon limit

In [16] the Hofman-Maldacena (HM) limit was argued in the case of the elliptic solution (2.13) to correspond to taking the elliptic moduli  $k$  to unity, while at the same time scaling

the world-sheet coordinates by letting  $\kappa \rightarrow \infty$ . However, the limit  $\kappa \rightarrow \infty$  is actually forced upon us when we take the limit  $k \rightarrow 1$ , as can be seen from equation (2.23). It follows that the HM limit is simply

$$\text{HM limit : } k \rightarrow 1.$$

But taking the elliptic modulus  $k$  to unity is equivalent to taking the complementary elliptic modulus  $k' = \sqrt{1 - k^2}$  to zero, which from its definition in (A.1) means that in this limit the branch points  $x_1$  and  $x_2$  merge. This in turn is equivalent to the pinching of a particular  $b$ -cycle of the curve. However, keeping the solution real as we take this limit requires that the conjugate branch points  $\bar{x}_1$  and  $\bar{x}_2$  also merge, so that one should also pinch another particular  $b$ -cycle. To understand what happens to the curve in this degeneration consider

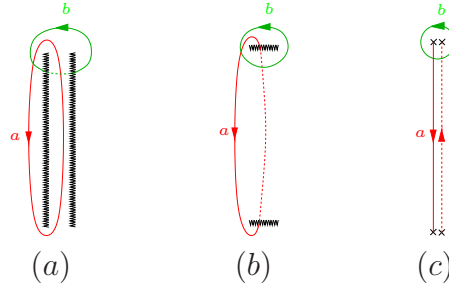


Figure 4: (a) Neighbouring branch cuts on  $\Sigma$ . (b) The same elliptic curve with the branch cuts chosen differently. (c) The singular limit  $\Sigma_{\text{sing}}$  of  $\Sigma$ .

the situation when  $x_1$  is very close to  $x_2$ ,  $|x_1 - x_2| \ll 1$  (see Figure 4 (a)). As the branch points merge in pairs ( $x_1$  with  $x_2$  and  $\bar{x}_1$  with  $\bar{x}_2$ ), the branch cuts (which can be freely chosen to connect pairs of branch points which are merging, see Figure 4 (b)) disappear and leave behind singular points at the now coalescing branch points  $x_1 = x_2$  and  $\bar{x}_1 = \bar{x}_2$ . In the limit, a homology  $a$ -cycle joins the singular points  $x_1$  and  $\bar{x}_1$  on the top sheet and goes back from  $\bar{x}_1$  to  $x_1$  on the bottom sheet, whereas a homology  $b$ -cycle circles the singular point  $x_1$  on the top sheet (see Figure 4 (c)).

Since the period  $T_x$  of a ‘single-hop’ defined in (2.24) blows up in the singular curve limit  $k \rightarrow 1$ , this means that as the elliptic curve  $\Sigma$  degenerates to a singular curve the restriction of the corresponding periodic two-gap solution (2.13) to the ‘single-hop’ in (2.25) turns into a soliton solution on the real line  $x \in \mathbb{R}$ . Indeed, the  $k \rightarrow 1$  limit of the two-gap solution (2.13) looks like

$$Z_1 = \frac{\cos(\tilde{\rho}_-)}{\cosh(\tilde{X})} e^{iv_+ \tilde{T} + i\varphi_1^0}, \quad Z_2 = \frac{\sinh(\tilde{X} - i\tilde{\rho}_-)}{\cosh(\tilde{X})} e^{i \tan(\tilde{\rho}_-) \tilde{X} + iv_- \tilde{T} + i\varphi_2^0}, \quad (3.1)$$

where  $v_-^2 - v_+^2 = \text{dn}^2(i\tilde{\rho}_-, 1) = 1 + \tan^2 \tilde{\rho}_-$ . Using the periodicity condition (2.27) it follows that (keeping the ratio  $\frac{N_-}{n}$  finite but  $\frac{N_+}{n} \sim K$  in the limit  $k \rightarrow 1$ )

$$v = \frac{\tan \tilde{\rho}_-}{v_-}, \quad v_+ = \tan \alpha,$$

for some  $\alpha \in \mathbb{R}$ , so that (after scaling the coordinates  $(x, t) \rightarrow (\cos(\alpha) x, \cos(\alpha) t)$  by a finite quantity) equation (3.1) yields exactly the dyonic giant magnon solution (again after the interchange of coordinates  $Z_1 \leftrightarrow Z_2$ )

$$\begin{aligned} Z_1 &= \frac{1}{\sqrt{1 + \tilde{k}^2}} \frac{1}{\cosh(\cos(\alpha) \tilde{X})} e^{i \sin(\alpha) \tilde{T} + i \varphi_1^0}, \\ Z_2 &= \frac{1}{\sqrt{1 + \tilde{k}^2}} \left[ \tanh(\cos(\alpha) \tilde{X}) - i \tilde{k} \right] e^{i t + i \varphi_2^0}. \end{aligned}$$

with  $\tilde{k} \equiv \tan \tilde{\rho}_-$ .

The global charges of this dyonic giant magnon solution are obtained as the  $k \rightarrow 1$  limits of the global charges (2.16) of the elliptic solution. If we defined the charges  $\mathcal{J}_1, \mathcal{J}_2$  and energy  $\mathcal{E}$  attributed to a ‘single-hop’ by

$$\mathcal{J}_i = \frac{J_i}{n}, \quad i = 1, 2, \quad \mathcal{E} = \frac{E}{n} = \kappa \frac{\sqrt{\lambda}}{n},$$

then we may write down the following linear combinations which remain finite as  $k \rightarrow 1$

$$\begin{aligned} \mathcal{E} - \mathcal{J}_1 &= \frac{\sqrt{\lambda}}{4\pi} \left| \left( x_1 - \frac{1}{x_1} \right) - \left( \bar{x}_1 - \frac{1}{\bar{x}_1} \right) \right|, \\ \mathcal{J}_2 &= \frac{\sqrt{\lambda}}{4\pi} \left| \left( x_1 + \frac{1}{x_1} \right) - \left( \bar{x}_1 + \frac{1}{\bar{x}_1} \right) \right|, \end{aligned} \tag{3.2}$$

which follow from (2.20) and (2.17) respectively, using the expression for  $dp$  (on the top sheet) in the singular limit

$$dp(x) = \frac{\pi \kappa dx}{(x - x_1)(x - \bar{x}_1)} \left[ \frac{|1 - x_1|^2}{(x - 1)^2} + \frac{|1 + x_1|^2}{(x + 1)^2} \right].$$

We also define the giant magnon momentum as

$$\mathfrak{p} \equiv \pi - 2\tilde{\rho}_- = 2\pi \int_{\infty^+}^{0^+} \nu / \int_b \nu = -i \ln \left( \frac{x_1}{\bar{x}_1} \right), \tag{3.3}$$

where the last two equalities follow from the singular limit  $k \rightarrow 1$  of the second equation in (2.2) and using  $K'(1) = \frac{\pi}{2}$ . The dyonic giant magnon dispersion relation follows immediately from (3.2) and (3.3), namely

$$\mathcal{E} - \mathcal{J}_1 = \sqrt{\mathcal{J}_2^2 + \frac{\lambda}{\pi^2} \sin^2 \frac{\mathfrak{p}}{2}}.$$

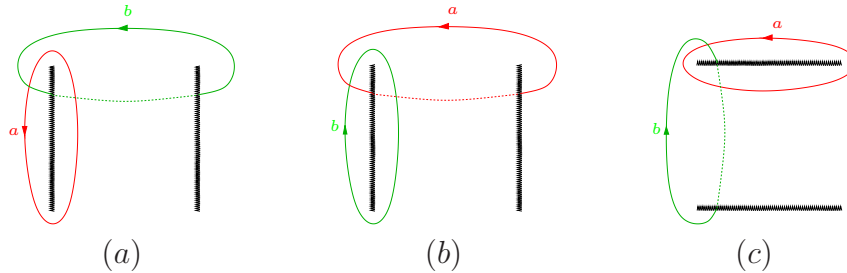


Figure 5: (a) The elliptic curve  $\Sigma$  with its 4 branch points and its canonical  $a$ - and  $b$ -cycles of  $H_1(\Sigma)$ . (b) The same elliptic curve after applying the automorphism which has the following action  $a \mapsto b, b \mapsto -a$  on  $H_1(\Sigma)$ . Note that the branch points are unchanged since the curve is mapped to itself. (c) Since the branch cuts are purely a matter of choice, it is convenient to redefine them so as to make the new  $a$ - and  $b$ -cycles take their standard form on  $\Sigma$ .

### 3.2 Connection with condensate cuts

In this section we mention the connection between the above construction of giant magnons as singular limits of finite-gap solutions with the construction of giant magnons in terms of curves with ‘condensate cuts’ [8].

Recall that in the finite-gap integration method we have an elliptic curve  $\Sigma$  equipped with a normalised meromorphic 1-form  $dp$  with the following periods

$$\int_a dp = 0, \quad \int_b dp = 2\pi n, \quad n \in \mathbb{Z}.$$

The vanishing of the  $a$ -periods of  $dp$  guarantees that the Abelian integral  $p(x) = \int^{x^+} dp$  is a well define and single valued function on the top sheet. If the  $a$ -periods of  $dp$  were non-vanishing, a condensate cut would be needed on  $\Sigma$  in order to define a single valued domain of the differential  $dp$  on the top sheet of  $\Sigma$ . In this sense condensate cuts are due to non-zero  $a$ -periods of  $dp$  (the terminology comes from the gauge theory side; see for instance [9]). It is important to note however that condensate cuts are not a property of the elliptic curve  $\Sigma$  but rather of the Abelian differential  $dp$  living on  $\Sigma$ . In order to obtain the condensate cut picture of giant magnons of [8], one could at this stage apply the modular transformation  $\tau \mapsto -\frac{1}{\tau}$  which has the effect of swapping around the  $a$ - and  $b$ -cycles as  $a \mapsto b, b \mapsto -a$  (see Figure 5) so that the differential  $dp$  now satisfies

$$\int_b dp = 0, \quad \int_a dp = 2\pi n, \quad n \in \mathbb{Z}.$$

Notice that the Abelian integral  $p(x) = \int^{x^+} dp$  does not define a single valued function on the top sheet anymore. One must introduce a ‘condensate cut’  $c$  on the top sheet to define a single branch of this multivalued function. This cut should intersect the  $a$ -cycle once, which can be achieved by connecting the branch cuts of  $\Sigma$  (see Figure 6).

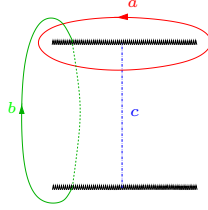


Figure 6: Artificial ‘condensate cut’  $c$  for  $dp$ .

Shrinking the  $b$ -period in the original picture of Figure 5 ( $a$ ) now corresponds to shrinking the  $a$ -period in Figure 6 to a point. In particular, the  $k \rightarrow 1$  limit of the curve which takes  $x_1 \rightarrow x_2$  (and  $\bar{x}_1 \rightarrow \bar{x}_2$ ) leaves behind a condensate cut on  $\Sigma$ , connecting the two singular points  $x_1 = x_2, \bar{x}_1 = \bar{x}_2$ . This picture of course is no different to the one we used in section 3.1, where the non-vanishing  $b$ -cycle around  $x_1 = x_2$  could equally be interpreted as a ‘condensate’ connecting  $x_1 = x_2$  to  $\bar{x}_1 = \bar{x}_2$ . A multivalued function  $f$  on the top sheet can be described in two equivalent ways: either using condensate cuts or by stating that  $\int_c df \neq 0$  for some closed curve  $c$  lying entirely on the top sheet. In the case of the quasi-momentum  $p(x)$ , the conditions that  $\oint_{x_1} dp \neq 0$  and  $\oint_{\bar{x}_1} dp \neq 0$  can be accounted for by requiring  $p(x)$  to have simple poles at  $x_1$  and  $\bar{x}_1$ , as was done in [8].

## Acknowledgements

I would like to thank Keisuke Okamura and Ryo Suzuki for interesting discussions. This work is supported by EPSRC.

## A Elliptic setup

Throughout these appendices we will be relying heavily on the book by Byrd and Friedman [24] for computations of elliptic integrals, and so we adopt the convention that any equation reference of the form “xxx.yy” refers to an equation in this book. Part of the calculation parallels that in [25].

In order to simplify things, we first seek the Möbius transformation that sends three of the branch points to the real axis, for instance  $x_2 \rightarrow 0, x_1 \rightarrow 1, \bar{x}_2 \rightarrow \infty$ , which is easily found to be

$$w(x) = \frac{x - x_2}{h(x - \bar{x}_2)}, \quad h \equiv \frac{x_1 - x_2}{x_1 - \bar{x}_2}. \quad (\text{A.1})$$

In the  $w$ -plane the branch point  $\bar{x}_1$  gets mapped to the real line

$$w(\bar{x}_1) = \frac{1}{|h|^2} = (k')^{-2}, \quad k' \equiv |h| \in \mathbb{R},$$

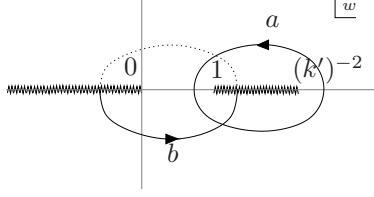


Figure 7:  $a$ - and  $b$ -periods in  $w$ -plane.

as it should be since the branch points  $x_1, \bar{x}_1, x_2, \bar{x}_2$  are concentric in the  $x$ -plane. Note that  $k' < 1$  follows from our choice of putting both roots  $x_1, x_2$  in the upper-half of the  $x$ -plane; see Figure 7.

The inverse of (A.1) is given by

$$x(w) = \frac{x_2 - \bar{x}_2 hw}{1 - hw}, \quad (\text{A.2})$$

and so given any  $x_0 \neq \bar{x}_2$  such that  $w_0 = w(x_0) \neq \infty$  one can show that

$$x - x_0 = \frac{h(x_2 - \bar{x}_2)(w - w_0)}{(1 - hw)(1 - hw_0)}, \quad (\text{A.3a})$$

and in the limit  $w_0 \rightarrow \infty$  we obtain also

$$x - \bar{x}_2 = \frac{x_2 - \bar{x}_2}{1 - hw}. \quad (\text{A.3b})$$

Using (A.3) and after a little algebra we can reexpress the curve (2.1) in the  $w$ -coordinate

$$y^2 = -h^2 |x_1 - \bar{x}_2|^2 \left( \frac{x_2 - \bar{x}_2}{(1 - hw)^2} \right)^2 w(w - 1)(1 - (k')^2 w). \quad (\text{A.4})$$

Also, equation (A.2) can be used to derive

$$dx = \frac{h(x_2 - \bar{x}_2)}{(1 - hw)^2} dw. \quad (\text{A.5})$$

Before proceeding, we must first specify a branch for the function  $y$  that we will be working with. We do this by requiring that  $\text{Re } y > 0$  along the path  $a_1$  in Figure 8, which lies just below the cut from 1 to  $(k')^{-2}$  in the  $w$ -plane. As we move along the path  $a_1$  we have  $\text{Im}(dx) < 0$  and  $\text{Re}(dw) > 0$  so that (A.5) implies

$$\text{Re} \left( \frac{h}{(1 - hw)^2} \right) < 0,$$

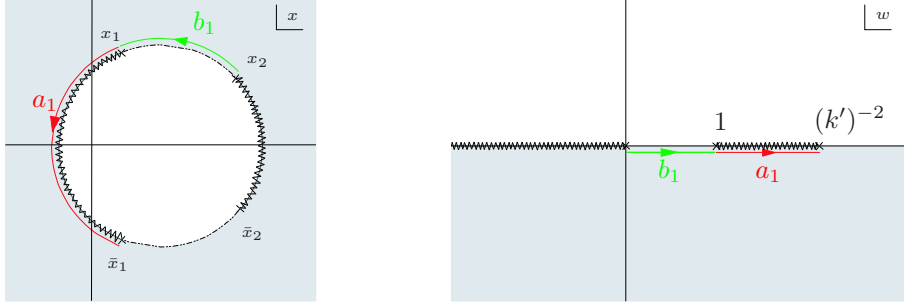


Figure 8: Choice of branch for  $y$ .

and since  $w(w-1)(1-(k')^2w) > 0$  for  $w \in [1, (k')^{-2}]$  we find

$$y = -|(x_1 - \bar{x}_2)(x_2 - \bar{x}_2)| \frac{h}{(1-hw)^2} \sqrt{w(w-1)(1-(k')^2w)}, \quad (\text{A.6})$$

where  $z \rightarrow \sqrt{z}$  denotes the principal branch of the square root (i.e. the branch  $\arg z \in (-\pi, \pi]$  on which  $\text{Re}\sqrt{z} > 0$ ). We can now obtain a simple expression for the unique (up to a multiplicative constant) holomorphic differential on the elliptic curve, namely

$$\nu \equiv \frac{dx}{y} = \frac{-i}{|x_1 - \bar{x}_2|} \frac{dw}{\sqrt{w(w-1)(1-(k')^2w)}}. \quad (\text{A.7})$$

Expressed in the  $w$ -coordinate it is simple to obtain the  $a$ - and  $b$ -periods of  $\nu$  in terms of elliptic functions. For instance, since the value of (A.6) has opposite sign on either side of the cut from 1 to  $(k')^{-2}$ , the  $a$ -period is just twice the integral along the curve  $a_1$  in Figure 8, which using 236.00 can be expressed in terms of standard elliptic functions

$$\int_a \nu = \frac{-2i}{|x_1 - \bar{x}_2|} \int_1^{(k')^{-2}} \frac{dw}{\sqrt{w(w-1)(1-(k')^2w)}} = \frac{-4iK}{|x_1 - \bar{x}_2|}, \quad K \equiv K(k),$$

where  $k \equiv \sqrt{1-(k')^2}$  is the complementary modulus to  $k'$ . It is thus natural to define the unique normalised holomorphic differential as follows

$$\omega \equiv -\frac{|x_1 - \bar{x}_2|}{4iK} \nu. \quad (\text{A.8})$$

Similarly the  $b$ -period is twice the integral along the curve  $b_1$  lying just below the real axis as shown in Figure 8. However, one must be careful in dealing with the branch of the square root, so that for instance one has

$$\sqrt{w(w-1)(1-(k')^2w)} = -i\sqrt{w(1-w)(1-(k')^2w)} \quad \text{for } w \in b_1.$$

Equation 234.00 then leads to

$$\int_b \nu = \frac{-2i}{|x_1 - \bar{x}_2|} \int_0^1 \frac{dw}{-i\sqrt{w(1-w)(1-(k')^2w)}} = \frac{4K'}{|x_1 - \bar{x}_2|}, \quad K' \equiv K(k').$$

The period matrix in the elliptic case is simply a number given here by

$$\Pi = \int_b \omega = -\frac{|x_1 - \bar{x}_2|}{4iK} \int_b \nu = \frac{iK'}{K} \equiv \tau.$$

## B $\Theta$ -functions

To compute  $\int_{\infty^\pm} \omega$  which appear inside the  $\theta$ -functions appearing in (1.8) we will evaluate the integrals  $\int_{\infty^-} \omega$  and  $\int_{0^-} \omega$  since

$$\int_{\infty^\pm} \omega = \frac{1}{2} \left( \int_{0^-} \omega \mp \int_{\infty^-} \omega \right). \quad (\text{B.1})$$

Such a decomposition is useful because an integral of the form  $\int_{x^-}^{x^+} \omega$  can be related to the  $b$ -periods of a normalised Abelian differential of the third kind  $\omega_x$  with only poles at  $x^\pm$  and defined uniquely by its residues there

$$\int_a \omega_x = 0, \quad \text{res}_{x^\pm} \omega_x = \pm \frac{1}{2\pi i}. \quad (\text{B.2})$$

More precisely, what one can show using the Riemann bilinear identities is that

$$\int_{x^-}^{x^+} \omega = \int_b \omega_x.$$

To compute the  $b$ -periods of  $\omega_0$  and  $\omega_\infty$  we need explicit expressions for these differentials. However, since they are both uniquely defined by the conditions (B.2), if we can explicitly construct differentials satisfying (B.2) we are done. But  $-\frac{x}{2\pi i}\nu$  has the right residues<sup>8</sup> at  $x = \infty$  and  $\frac{y(0)}{2\pi i x}\nu$  the right residues at  $x = 0$  so all we need to do is normalise these differentials (i.e. subtract multiples of the holomorphic differential  $\nu$  to make their  $a$ -periods vanish), so that

$$\omega_\infty = -\frac{1}{2\pi i} (x - L_\infty) \nu, \quad \omega_0 = \frac{y(0)}{2\pi i} \left( \frac{1}{x} - L_0 \right) \nu, \quad (\text{B.3})$$

---

<sup>8</sup>This is because  $-\frac{x}{2\pi i}\nu = -\frac{x}{2\pi i}\frac{dx}{y}$  and  $y \sim_{x \rightarrow \infty} x^2$  (since  $\text{Re } y(x) > 0$  for large  $x \in \mathbb{R}$  by our choice of branch for  $y$ ) so that  $-\frac{x}{2\pi i}\nu = -\frac{1}{2\pi i}\frac{dx}{x} = \frac{1}{2\pi i}\frac{d\lambda}{\lambda}$  where  $\lambda = \frac{1}{x}$  is a local parameter near  $x = \infty$ .



where we have defined

$$L_\infty \equiv \frac{\int_a x \nu}{\int_a \nu}, \quad L_0 \equiv \frac{\int_a \frac{1}{x} \nu}{\int_a \nu}. \quad (\text{B.4})$$

Using equations (A.3b) and (A.7) we can write

$$\begin{aligned} \int_b x \nu &= \frac{-2i}{|x_1 - \bar{x}_2|} \int_0^1 \left( \bar{x}_2 + \frac{x_2 - \bar{x}_2}{1 - hw} \right) \frac{dw}{-i\sqrt{w(1-w)(1-(k')^2w)}}, \\ \int_b \frac{1}{x} \nu &= \frac{-2i}{|x_1 - \bar{x}_2|} \int_0^1 \left( \frac{1}{\bar{x}_2} + \frac{1}{\bar{x}_2} \frac{x_2 - \bar{x}_2}{\bar{x}_2 hw - x_2} \right) \frac{dw}{-i\sqrt{w(1-w)(1-(k')^2w)}}. \end{aligned}$$

The second summands in both of these integrals can be reduced to canonical elliptic functions using 233.02, whereas the first summands are proportional to  $\int_b \nu$  which has already been computed. So we end up with

$$\int_{\infty^-}^{\infty^+} \omega = \int_b \omega_\infty = \frac{-1}{2\pi i} \frac{4}{|x_1 - \bar{x}_2|} [(\bar{x}_2 - L_\infty)K' + (x_2 - \bar{x}_2)\Pi(h, k')], \quad (\text{B.5a})$$

$$\int_{0^-}^{0^+} \omega = \int_b \omega_0 = \frac{y(0)}{2\pi i} \frac{4}{|x_1 - \bar{x}_2|} \left[ \left( \frac{1}{\bar{x}_2} - L_0 \right) K' + \left( \frac{1}{x_2} - \frac{1}{\bar{x}_2} \right) \Pi(k, k') \right], \quad (\text{B.5b})$$

where  $h_2 \equiv h \frac{\bar{x}_2}{x_2} = w(0)^{-1}$ ,  $w(x)$  being the Möbius transformation (A.1) to the  $w$ -plane. Although these integrals look complicated, it turns out that their real parts are very simple. They can be computed using the addition formula 117.02 for elliptic functions of the third kind  $\Pi(h, k')$ , after noting the relations  $\bar{h} = (k')^2/h$  and  $\bar{h}_2 = (k')^2/h_2$  between their arguments.

If we assume that the two cuts are on either side of the origin  $x = 0$  then it follows from our choice of branch for  $y$  that  $y(0) = -|x_1||x_2| < 0$ : indeed, all along the real axis  $y \in \mathbb{R}$ , but  $y(x) > 0$  when  $x$  lies outside the region in between the two cuts, and  $y(x) < 0$  when  $x$  lies between the two cuts. After some algebra we find

$$\text{Re} \left( \int_{\infty^-}^{\infty^+} \omega \right) = \frac{1}{2} \int_{\infty^-}^{\infty^+} (\omega + \bar{\omega}) = -\frac{1}{2}, \quad \text{Re} \left( \int_{0^-}^{0^+} \omega \right) = \frac{1}{2} \int_{0^-}^{0^+} (\omega + \bar{\omega}) = \frac{1}{2}.$$

Equation (2.2) in the text now follows immediately from this and equation (B.1).

We now verify that the variables  $\rho_\pm \in \mathbb{R}$  in (2.2) together represent an extra degree of freedom of the solution that cannot be obtained simply from the modulus  $k'$  of the curve. For this we will find simpler expressions for (B.5). The quantities  $L_\infty, L_0$  defined in (B.4) can be computed explicitly using 236.00, 236.02 and the fact that  $L_\infty, L_0 \in \mathbb{R}$  (or equivalently using 117.03); after some algebra one finds

$$L_\infty = x_2 + (x_2 - \bar{x}_2) \frac{h}{1-h} \frac{\Pi(\beta^2, k)}{K}, \quad \beta^2 \equiv \frac{k^2}{1-h}. \quad (\text{B.6a})$$

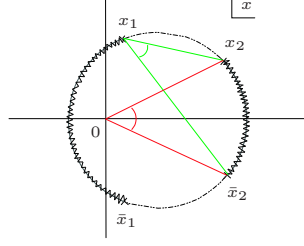


Figure 9:  $y(0) < 0 \Leftrightarrow \text{Arg } h_2 \in (-\pi, 0)$ .

$$L_0 = \frac{1}{x_2} + \left( \frac{1}{x_2} - \frac{1}{\bar{x}_2} \right) \frac{h_2}{1-h_2} \frac{\Pi((\beta')^2, k)}{K}, \quad (\beta')^2 \equiv \frac{k^2}{1-h_2}. \quad (\text{B.6b})$$

Now using the addition formula 117.05 we can relate  $\Pi(h, k')$  which appears in (B.5a) to  $\Pi(\beta^2, k)$  which appears in (B.6a) on the one hand and  $\Pi(h_2, k')$  which appears in (B.5b) to  $\Pi((\beta')^2, k)$  which appears in (B.6b) on the other

$$(h-1)K\Pi(h, k') + hK'\Pi(\beta^2, k) + (1-h)KK' = \frac{\pi}{2} \sqrt{\frac{1-h}{h-1}} F(\phi, k'), \quad (\text{B.7a})$$

$$(h_2-1)K\Pi(h_2, k') + h_2K'\Pi((\beta')^2, k) + (1-h_2)KK' = \frac{\pi}{2} \sqrt{\frac{1-h_2}{h_2-1}} F(\phi', k'), \quad (\text{B.7b})$$

where

$$\phi \equiv \sin^{-1} \left( \frac{\sqrt{h}}{k'} \right), \quad \phi' \equiv \sin^{-1} \left( \frac{\sqrt{h_2}}{k'} \right). \quad (\text{B.8})$$

Note that each square root in these expressions is taken to be the principal branch of the square root as previously defined. Equations (B.7) lead to great simplifications in (B.5), and after the dust settles we end up with

$$\int_{\infty^-}^{\infty^+} \omega = -i \frac{x_2 - \bar{x}_2}{|x_1 - \bar{x}_2|} \frac{1}{1-h} \sqrt{\frac{1-h}{h-1}} \frac{F(\phi, k')}{K}, \quad (\text{B.9a})$$

$$\int_{0^-}^{0^+} \omega = -i \frac{y(0)}{|x_2|^2} \frac{x_2 - \bar{x}_2}{|x_1 - \bar{x}_2|} \frac{1}{1-h_2} \sqrt{\frac{1-h_2}{h_2-1}} \frac{F(\phi', k')}{K}. \quad (\text{B.9b})$$

To simplify this expression further one must be careful in dealing with the square roots. We must deal separately with two cases: (1) when  $x = 0$  lies between the two cuts on the one hand, and (2) when  $x = 0$  lies outside the two cuts on the other (we deal with this last case as well for completeness).

In case (1) we have  $y(0) < 0$  and it is not too hard to show that  $\text{Arg } h_2 \in (-\pi, 0)$  (see Figure 9) so that  $\text{Arg}((1 - h_2)/(\bar{h}_2 - 1)) \in (-\pi, 0)$  which implies

$$\underline{\text{case (1)}} : \quad \frac{1}{1 - h_2} \sqrt{\frac{1 - h_2}{\bar{h}_2 - 1}} = \frac{-i}{|1 - h_2|}.$$

In case (2) we have  $y(0) > 0$  and now one can show that  $\text{Arg } h_2 \in (0, \pi)$  (see Figure 9) so that this time we have  $\text{Arg}((1 - h_2)/(\bar{h}_2 - 1)) \in (0, \pi)$  which implies

$$\underline{\text{case (2)}} : \quad \frac{1}{1 - h_2} \sqrt{\frac{1 - h_2}{\bar{h}_2 - 1}} = \frac{i}{|1 - h_2|}.$$

Thus, in both cases we can write

$$\frac{1}{1 - h} \sqrt{\frac{1 - h}{\bar{h} - 1}} = \frac{i}{|1 - h|}, \quad \frac{y(0)}{1 - h_2} \sqrt{\frac{1 - h_2}{\bar{h}_2 - 1}} = \frac{i|x_1||x_2|}{|1 - h_2|}.$$

Plugging these expressions back into the equations (B.9) we finally obtain

$$\int_{\infty^-}^{\infty^+} \omega = i \frac{F(\phi, k')}{K}, \tag{B.10a}$$

$$\int_{0^-}^{0^+} \omega = i \frac{F(\phi', k')}{K}. \tag{B.10b}$$

We are now in a position to obtain explicit expressions for  $\rho_{\pm}$  by making use of formula 116.01 to obtain the sum and the difference of (B.10a) and (B.10b) given in (B.1). The result is given in (2.5) and (2.6), where the fact that  $\sqrt{\bar{h} - 1} = -i\sqrt{1 - \bar{h}}$  and  $\sqrt{h_2 - 1} = i\sqrt{1 - h_2}$  has been used to obtain (2.6).

## C Exponentials

For the evaluation of the integrals  $\int_{\infty^{\pm}}^{0^+} d\mathcal{Q}$  this we will start by evaluating the integrals  $\int_{\infty^-}^{\infty^+} d\mathcal{Q}$  and  $\int_{0^-}^{0^+} d\mathcal{Q}$  since

$$\int_{\infty^{\pm}}^{0^+} d\mathcal{Q} = \frac{1}{2} \left( \int_{0^-}^{0^+} d\mathcal{Q} \mp \int_{\infty^-}^{\infty^+} d\mathcal{Q} \right).$$

As in (B.1) we can relate the integral  $\int_{x^-}^{x^+} d\mathcal{Q}$  for general  $x$  to the third kind Abelian differential  $\omega_x$  defined by (B.2). To do this we will again make use of the Riemann bilinear

identities but this time for the differentials  $dp$  (or  $dq$ ) and  $\omega_x$ , thus obtaining

$$\int_{x^-}^{x^+} dp = - \sum \text{res } p(2\pi i \omega_x), \quad \int_{x^-}^{x^+} dq = - \sum \text{res } q(2\pi i \omega_x).$$

Making use of equation (B.3) for  $\omega_\infty$  and  $\omega_0$  as well as (2.7) and (2.9) we can evaluate the residues in the last equations explicitly so that the integrals of  $d\mathcal{Q}$  reduce to

$$\int_{\infty^+}^{0^+} d\mathcal{Q} = -\frac{1+y(0)}{|x_1-\bar{x}_2|} \tilde{T} + \frac{L_\infty+y(0)L_0}{|x_1-\bar{x}_2|} (\tilde{X} - \tilde{X}_0), \quad (\text{C.1a})$$

$$\int_{\infty^-}^{0^+} d\mathcal{Q} = \frac{1-y(0)}{|x_1-\bar{x}_2|} \tilde{T} - \frac{L_\infty-y(0)L_0}{|x_1-\bar{x}_2|} (\tilde{X} - \tilde{X}_0). \quad (\text{C.1b})$$

Now using equations 117.05 and 110.10 (and with the help of (B.7)) one can show that the following hold

$$\frac{\Pi(\beta^2, k)}{K} = \frac{1}{h} \sqrt{\frac{1-h}{h-1}} \left[ Z_0(\phi, k') + \frac{\pi}{2} \frac{F(\phi, k')}{KK'} \right], \quad (\text{C.2a})$$

$$\frac{\Pi((\beta')^2, k)}{K} = \frac{1}{h_2} \sqrt{\frac{1-h_2}{h_2-1}} \left[ Z_0(\phi', k') + \frac{\pi}{2} \frac{F(\phi', k')}{KK'} \right], \quad (\text{C.2b})$$

where  $\phi, \phi'$  were defined in (B.8),  $\beta^2, (\beta')^2$  are defined in (B.7) and  $Z_0(\theta, k')$  is the Jacobi zeta-function defined as

$$Z_0(\theta, k') = E(\theta, k') - \frac{E'}{K'} F(\theta, k').$$

We can now use (C.2) to obtain

$$L_\infty = x_2 - |x_1 - \bar{x}_2| \left[ Z_0(\phi, k') + \frac{\pi}{2} \frac{F(\phi, k')}{KK'} \right], \quad (\text{C.3a})$$

$$y(0)L_0 = \frac{y(0)}{x_2} + |x_1 - \bar{x}_2| \left[ Z_0(\phi', k') + \frac{\pi}{2} \frac{F(\phi', k')}{KK'} \right]. \quad (\text{C.3b})$$

Using the addition formula 142.01 for Jacobi zeta-functions we find

$$\frac{L_\infty \mp y(0)L_0}{|x_1 - \bar{x}_2|} = \frac{x_2 \mp \frac{y(0)}{x_2}}{|x_1 - \bar{x}_2|} - \sqrt{h} \sqrt{h_2} \sin \varphi_\pm \mp \left[ Z_0(\varphi_\pm, k') + \frac{\pi}{2} \frac{F(\varphi_\pm, k')}{KK'} \right].$$

Now using 143.02 for Jacobi zeta-functions with imaginary arguments (and also 126.01 for Jacobian elliptic functions with imaginary arguments) we can write the expression in square brackets in the last expression as

$$\left[ Z_0(u_\pm, k') + \frac{\pi}{2} \frac{u_\pm}{KK'} \right] = iZ_0(iu_\pm, k) + \tan \varphi_\pm \sqrt{1 - (k')^2 \sin^2 \varphi_\pm},$$

where  $u_{\pm} = F(\varphi_{\pm}, k') = \text{am}^{-1}(\varphi_{\pm}, k')$ , and  $Z_0(u_{\pm}, k') = Z_0(\varphi_{\pm}, k')$  is just a standard change in notation of the argument. Grouping everything together we obtain,

$$\mp \frac{L_{\infty} \mp y(0)L_0}{|x_1 - \bar{x}_2|} = iZ_0(iu_{\pm}, k) \mp \left[ \frac{x_2 \mp \frac{y(0)}{x_2}}{|x_1 - \bar{x}_2|} - \sqrt{h}\sqrt{h_2} \sin \varphi_{\pm} \mp \tan \varphi_{\pm} \sqrt{1 - (k')^2 \sin^2 \varphi_{\pm}} \right]. \quad (\text{C.4})$$

Everything in the square bracket of this last expression can be expressed in terms of the branch points  $\{x_1, \bar{x}_1, x_2, \bar{x}_2\}$  by making use of (2.6),

$$\begin{aligned} \tan \varphi_{\pm} &= \mp \frac{|x_1 - \bar{x}_2|}{\sqrt{x_1 x_2} \pm \sqrt{\bar{x}_1 \bar{x}_2}}, \\ \sin \varphi_{\pm} &= \frac{|x_1 - \bar{x}_2|}{|x_2| \mp |x_1|}, \\ \sqrt{1 - (k')^2 \sin^2 \varphi_{\pm}} &= \pm \frac{\sqrt{\bar{x}_1 x_2} \pm \sqrt{x_1 \bar{x}_2}}{|x_2| \pm |x_1|}. \end{aligned}$$

Note that to obtain the right sign in the last of these expressions one needs to use the fact that  $\sqrt{x_1 \bar{x}_2} + \sqrt{\bar{x}_1 x_2}$  is real and positive. We also assume that  $|x_1| \geq |x_2|$  and that  $x = 0$  lies between the two cuts. After simplifying the expression in the square bracket of (C.4) one finds (including the overall “ $\mp$ ” sign sitting outside the square bracket)

$$-\frac{(|x_2| \pm |x_1|)(\sqrt{\bar{x}_1 x_2} \pm \sqrt{x_1 \bar{x}_2})}{|x_1 - \bar{x}_2|(\sqrt{x_1 x_2} \pm \sqrt{\bar{x}_1 \bar{x}_2})} = \frac{\tan \varphi_{\pm} \sqrt{1 - (k')^2 \sin^2 \varphi_{\pm}}}{\sin^2 \varphi_{\pm}} = i \text{cs}(iu_{\pm}, k) \text{dn}(iu_{\pm}, k),$$

where use was made of 125.02 for Jacobi elliptic functions with imaginary arguments. Now one of the equations among 141.01 implies the following

$$Z_0(iu_{\pm}, k) + \text{cs}(iu_{\pm}, k) \text{dn}(iu_{\pm}, k) = Z_0(iu_{\pm} + iK', k) + \frac{i\pi}{2K} \equiv Z_1(iu_{\pm}, k),$$

where the last equality is the definition of the Jacobi zeta-function  $Z_1$ . So finally,

$$\mp \frac{L_{\infty} \mp y(0)L_0}{|x_1 - \bar{x}_2|} = iZ_1(iu_{\pm}, k). \quad (\text{C.5})$$

Using  $u_+ = F(\varphi_+, k') = \tilde{\rho}_- + K'$ , equation (C.5) gives in the “+” sign case

$$-\frac{L_{\infty} - y(0)L_0}{|x_1 - \bar{x}_2|} = iZ_1(iu_+, k) = iZ_1(i\tilde{\rho}_- + K', k).$$

Now plugging this back into (C.1b) yields

$$-i \int_{\infty^-}^{0^+} d\mathcal{Q} = -i \frac{1 - y(0)}{|x_1 - \bar{x}_2|} \tilde{T} + Z_1(i\tilde{\rho}_- + K', k) (\tilde{X} - \tilde{X}_0),$$

and since  $\frac{i}{2} \int_b d\mathcal{Q} = \frac{i\pi}{2K}(\tilde{X} - \tilde{X}_0)$  it follows that the exponent in (2.4b) can be written

$$-i \int_{\infty^-}^{0^+} d\mathcal{Q} + \frac{i}{2} \int_b d\mathcal{Q} = Z_0(i\tilde{\rho}_-, k) (\tilde{X} - \tilde{X}_0) - i \frac{1 - y(0)}{|x_1 - \bar{x}_2|} \tilde{T}. \quad (\text{C.6})$$

In the “−” sign case, using  $iu_- = iF(\varphi_-, k') = K + i\tilde{\rho}_+$ , equation (C.5) yields

$$\frac{L_\infty + y(0)L_0}{|x_1 - \bar{x}_2|} = iZ_1(K + i\tilde{\rho}_+, k) = iZ_2(i\tilde{\rho}_+, k),$$

where the Jacobi zeta-functions  $Z_2$  is defined as

$$Z_2(u, k) = Z_1(u + K, k).$$

Equation (C.1a) then yields

$$-i \int_{\infty^+}^{0^+} d\mathcal{Q} = Z_2(i\tilde{\rho}_+, k) (\tilde{X} - \tilde{X}_0) + i \frac{1 + y(0)}{|x_1 - \bar{x}_2|} \tilde{T}. \quad (\text{C.7})$$

Defining the following variables

$$v_\pm = \frac{y(0) \pm 1}{|x_1 - \bar{x}_2|},$$

appearing in (C.6) and (C.7), it can be shown (using 122.03, 122.05 and 125.02) that they satisfy

$$v_-^2 - v_+^2 = \text{dn}^2(i\tilde{\rho}_-, k) + (k')^2 \text{sc}^2(i\tilde{\rho}_+, k).$$

## D Normalisation

Let us now turn to the evaluation of the constants  $h_\pm(0^+)$  and  $\chi(\infty^-)^{\frac{1}{2}}$  in the elliptic case at hand. Recall that  $h_\pm$  are meromorphic functions on  $\Sigma$  uniquely defined (up to normalisation) by having poles at the divisor  $\hat{\gamma}^+ = \hat{\gamma}_1^+ \cdot \hat{\gamma}_2^+$ , a zero at  $\infty^\pm$  and normalised by the conditions  $h_\pm(\infty^\mp) = 1$  respectively. From the general theory of Riemann surfaces we can then write expressions for these functions in terms of Riemann  $\theta$ -functions. This relies on Riemann’s theorem for the zeroes of a  $\theta$ -function, which states (in the elliptic case  $g = 1$ ) that if  $\theta(\mathcal{A}(P) - w)$  is not identically zero, then it has a single zero  $P_0$  (or a degree  $g$  divisor of zeroes in the general case) satisfying  $\mathcal{A}(P_0) = w - \mathcal{K}$ . So choosing  $w \equiv \mathcal{A}(Q_0) + \mathcal{K}$  yields  $\mathcal{A}(P_0 \cdot Q_0^{-1}) = 0$  which by Abel’s theorem implies  $P_0 = Q_0$ . So we can write  $h_\pm$  as follows

$$h_-(P) = \frac{\theta(\mathcal{A}(\infty^+) - w_1)\theta(\mathcal{A}(\infty^+) - w_2)}{\theta(\mathcal{A}(\infty^+) - w_-)\theta(\mathcal{A}(\infty^+) - w_0^-)} \frac{\theta(\mathcal{A}(P) - w_-)\theta(\mathcal{A}(P) - w_0^-)}{\theta(\mathcal{A}(P) - w_1)\theta(\mathcal{A}(P) - w_2)},$$

$$h_+(P) = \frac{\theta(\mathcal{A}(\infty^-) - w_1)\theta(\mathcal{A}(\infty^-) - w_2)}{\theta(\mathcal{A}(\infty^-) - w_+)\theta(\mathcal{A}(\infty^-) - w_0^+)} \frac{\theta(\mathcal{A}(P) - w_+)\theta(\mathcal{A}(P) - w_0^+)}{\theta(\mathcal{A}(P) - w_1)\theta(\mathcal{A}(P) - w_2)},$$

where

$$\begin{aligned}
w_i &\equiv \mathcal{A}(\hat{\gamma}_i^+) + \mathcal{K}, \quad i = 1, 2 \\
w_{\pm} &\equiv \mathcal{A}(\infty^{\pm}) + \mathcal{K}, \\
w_0^- &\equiv w_1 + w_2 - w_- = \mathcal{A}(\hat{\gamma}^+) - \mathcal{A}(\infty^-) + \mathcal{K} = D, \\
w_0^+ &\equiv w_1 + w_2 - w_+ = \mathcal{A}(\hat{\gamma}^+) - \mathcal{A}(\infty^+) + \mathcal{K} = D + \mathcal{A}(\infty^-).
\end{aligned}$$

One can absorb a lot of the common factors between  $h_{\pm}(0^+)$  into the overall constant  $C$  so that we are left with

$$\begin{aligned}
h_-(0^+) &= \frac{\theta(\mathcal{A}(\infty^+) - w_1)\theta(\mathcal{A}(\infty^+) - w_2)}{\theta(\mathcal{A}(\infty^+) - w_-)} \frac{\theta(\mathcal{A}(0^+) - w_0^-)}{\theta(\mathcal{A}(0^+) - w_+)} \\
h_+(0^+) &= \frac{\theta(\mathcal{A}(\infty^-) - w_1)\theta(\mathcal{A}(\infty^-) - w_2)}{\theta(\mathcal{A}(\infty^-) - w_+)} \frac{\theta(\mathcal{A}(0^+) - w_0^+)}{\theta(\mathcal{A}(0^+) - w_-)}.
\end{aligned} \tag{D.1}$$

Likewise, the function  $\chi(P)$  was defined as the unique meromorphic function with zeroes at the divisor  $\hat{\gamma}^+ \cdot \hat{\tau}\hat{\gamma}^+ = \hat{\gamma}_1^+ \cdot \hat{\gamma}_2^+ \cdot \hat{\tau}\hat{\gamma}_1^+ \cdot \hat{\tau}\hat{\gamma}_2^+$ , poles at the branch points given by the divisor  $B = B_1 \cdot B_2 \cdot \hat{\tau}B_1 \cdot \hat{\tau}B_2$  and normalised by the condition  $\chi(\infty^+) = 1$ , so that it can be constructed out of Riemann  $\theta$ -functions as follows

$$\begin{aligned}
\chi(P) &= \frac{\theta(\mathcal{A}(\infty^+) - b_1)\theta(\mathcal{A}(\infty^+) - b_2)\theta(\mathcal{A}(\infty^+) + \bar{b}_1)\theta(\mathcal{A}(\infty^+) + \bar{b}_2)}{\theta(\mathcal{A}(\infty^+) - w_1)\theta(\mathcal{A}(\infty^+) - w_2)\theta(\mathcal{A}(\infty^+) + \bar{w}_1)\theta(\mathcal{A}(\infty^+) + \bar{w}_2)} \\
&\quad \times \frac{\theta(\mathcal{A}(P) - w_1)\theta(\mathcal{A}(P) - w_2)\theta(\mathcal{A}(P) + \bar{w}_1)\theta(\mathcal{A}(P) + \bar{w}_2)}{\theta(\mathcal{A}(P) - b_1)\theta(\mathcal{A}(P) - b_2)\theta(\mathcal{A}(P) + \bar{b}_1)\theta(\mathcal{A}(P) + \bar{b}_2)}
\end{aligned}$$

where

$$b_i \equiv \mathcal{A}(B_i) + \mathcal{K}, \quad i = 1, 2$$

and we have used the fact that

$$\begin{aligned}
-\bar{w}_i &= -\overline{\mathcal{A}(\hat{\gamma}_i^+)} - \bar{\mathcal{K}}, = \mathcal{A}(\hat{\tau}\hat{\gamma}_i^+) + \mathcal{K}, \quad i = 1, 2, \\
-\bar{b}_i &= -\overline{\mathcal{A}(B_i)} - \bar{\mathcal{K}}, = \mathcal{A}(\hat{\tau}B_i) + \mathcal{K}, \quad i = 1, 2.
\end{aligned}$$

We thus obtain the following expression for the real constant  $\chi(\infty^-)^{\frac{1}{2}}$ ,

$$\chi(\infty^-)^{\frac{1}{2}} = \frac{|\theta(\mathcal{A}(\infty^+) - b_1)\theta(\mathcal{A}(\infty^+) - b_2)|}{|\theta(\mathcal{A}(\infty^+) - w_1)\theta(\mathcal{A}(\infty^+) - w_2)|} \frac{|\theta(\mathcal{A}(\infty^-) - w_1)\theta(\mathcal{A}(\infty^-) - w_2)|}{|\theta(\mathcal{A}(\infty^-) - b_1)\theta(\mathcal{A}(\infty^-) - b_2)|}. \tag{D.2}$$

Combining (D.1) and (D.2) and absorbing again some overall coefficient into the constant  $C$  we obtain up to a residual  $SU(2)_R \times SU(2)_L$  transformation (i.e. up to constant global phases)

$$\begin{aligned}
h_-(0^+) &= \frac{|\theta(\mathcal{A}(\infty^+) - b_1)\theta(\mathcal{A}(\infty^+) - b_2)|}{\theta(\mathcal{A}(\infty^+) - w_-)} \frac{\theta(\mathcal{A}(0^+) - w_0^-)}{\theta(\mathcal{A}(0^+) - w_+)} \\
\frac{h_+(0^+)}{\chi(\infty^-)^{\frac{1}{2}}} &= \frac{|\theta(\mathcal{A}(\infty^-) - b_1)\theta(\mathcal{A}(\infty^-) - b_2)|}{\theta(\mathcal{A}(\infty^-) - w_+)} \frac{\theta(\mathcal{A}(0^+) - w_0^+)}{\theta(\mathcal{A}(0^+) - w_-)}.
\end{aligned}$$

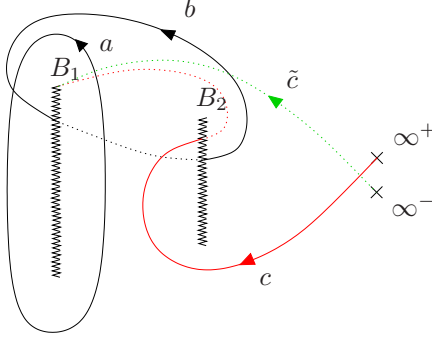


Figure 10: Curves  $c, \tilde{c}$  involved in computing  $\mathcal{A}(B_1)$  and  $\mathcal{A}(\infty^-) - \mathcal{A}(B_1)$ . Notice that neither of these two curves intersects the  $a$ - and  $b$ -cycles since they must lie within  $\Sigma_{\text{cut}}$ .

This is as much as we can simply these normalisation constants without explicitly evaluating them. To proceed we must now evaluate the arguments of each  $\theta$ -function in turn.

Now in the elliptic case there is just a single holomorphic 1-form  $\omega$  so that the formula (1.12) for  $\mathcal{K}$  simply yields  $\mathcal{K} = 2\pi \left( \frac{1}{2} + \frac{\tau}{2} \right)$ , and on the other hand we have  $D = 2\pi \left( \frac{1}{2} + X_0 \right)$ . We will also need to make use of (2.2) for the various integrals present. Using this information it is straightforward to show that

$$\begin{aligned}
\theta(\mathcal{A}(0^+) - w_0^-) &= \vartheta_3(X_0 - i\rho_+), \\
\theta(\mathcal{A}(0^+) - w_+) &= \exp\left(-\pi i \frac{\tau}{4} - \pi\rho_+\right) \vartheta_2(i\rho_+), \\
\theta(\mathcal{A}(0^+) - w_0^+) &= \exp\left(-\pi i \frac{\tau}{4} + \pi\rho_- + \frac{i}{2}D\right) \vartheta_1(X_0 - i\rho_-), \\
\theta(\mathcal{A}(0^+) - w_-) &= \vartheta_0(i\rho_-).
\end{aligned} \tag{D.3}$$

Next, one has  $\mathcal{A}(\infty^+) - w_- = -(\mathcal{A}(\infty^-) + \mathcal{K})$  and  $\mathcal{A}(\infty^-) - w_+ = \mathcal{A}(\infty^-) - \mathcal{K}$  where  $\mathcal{A}(\infty^-)$  can be evaluated in terms of (2.2) using (B.1) yielding  $\mathcal{A}(\infty^-) = 2\pi \left( \frac{1-\tau}{2} + i(\rho_+ - \rho_-) \right)$ . This immediately leads to

$$\theta(\mathcal{A}(\infty^+) - w_-) = \exp(\pi i \tau + 2\pi(\rho_+ - \rho_-)) \theta(\mathcal{A}(\infty^-) - w_+). \tag{D.4}$$

Finally we must obtain relations among the  $\theta$ -functions involving branch points. We have for instance

$$\mathcal{A}(B_1) = 2\pi \int_c \omega, \quad \mathcal{A}(\infty^-) - \mathcal{A}(B_1) = -2\pi \int_{\tilde{c}} \omega,$$

where the curves  $c, \tilde{c}$  are depicted in Figure 10. Recall that we had chosen a branch for the Abel integral  $\mathcal{A}(P) = 2\pi \int_{\infty^+}^P \omega$  by requiring that the path from  $\infty^+$  to  $P$  stayed within  $\Sigma_{\text{cut}}$ . This is insured by taking paths  $c$  that respect the following intersection numbers

$$c \cap a = c \cap b = 0.$$



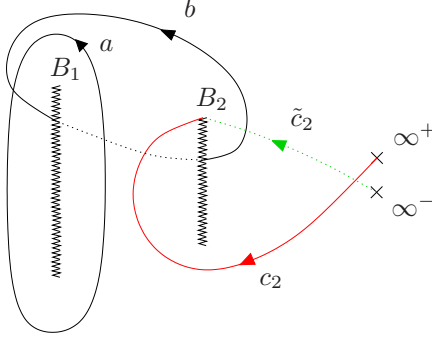


Figure 11: Curves  $c_2, \tilde{c}_2$  involved in computing  $\mathcal{A}(B_2)$  and  $\mathcal{A}(\infty^-) - \mathcal{A}(B_2)$ . Again, neither of these two curves intersects the  $a$ - and  $b$ -cycles since they must lie within  $\Sigma_{\text{cut}}$ .

The curves  $c, \tilde{c}$  are related by  $\hat{\sigma}c - b + a = \tilde{c}$ , which leads to (using also  $\hat{\sigma}^*\omega = -\omega$ )

$$\theta(\mathcal{A}(\infty^+) - b_1) = \theta(\mathcal{A}(\infty^-) - b_1). \quad (\text{D.5})$$

For the other branch point  $B_2$  things are very similar. In particular we have again

$$\mathcal{A}(B_2) = 2\pi \int_{c_2} \omega, \quad \mathcal{A}(\infty^-) - \mathcal{A}(B_2) = -2\pi \int_{\tilde{c}_2} \omega,$$

where the curves  $c_2, \tilde{c}_2$  are depicted in Figure 11. However, the curves  $c_2, \tilde{c}_2$  are now related by  $\hat{\sigma}c_2 + a = \tilde{c}_2$ , which leads to

$$|\theta(\mathcal{A}(\infty^+) - b_2)| = \exp\left(\pi i \frac{\tau}{2} + \pi(\rho_+ - \rho_-)\right) |\theta(\mathcal{A}(\infty^-) - b_2)|. \quad (\text{D.6})$$

So at last, gathering together equations (D.3), (D.4), (D.5), (D.6) and applying a global  $SU(2)_R \times SU(2)_L$  transformation to remove a relative phase  $\exp\left(\frac{i}{2}D\right)$  appearing in  $h_+(0^+)$  we obtain the expression (2.12) for the normalisation constants.

## References

- [1] D. M. Hofman and J. M. Maldacena, “Giant magnons,” J. Phys. A **39** (2006) 13095, arXiv:hep-th/0604135.
- [2] N. Dorey, “Magnon bound states and the AdS/CFT correspondence,” J. Phys. A **39** (2006) 13119, arXiv:hep-th/0604175.
- [3] N. Beisert, V. Dippel and M. Staudacher, “A novel long range spin chain and planar N = 4 super Yang-Mills,” JHEP **0407** (2004) 075, arXiv:hep-th/0405001.

- [4] M. Staudacher, “The factorized S-matrix of CFT/AdS,” JHEP **0505** (2005) 054, arXiv:hep-th/0412188.
- [5] N. Beisert and M. Staudacher, “Long-range PSU(2,2—4) Bethe ansaetze for gauge theory and strings,” Nucl. Phys. B **727** (2005) 1, arXiv:hep-th/0504190.
- [6] N. Beisert, “The su(2—2) dynamic S-matrix,” arXiv:hep-th/0511082.
- [7] H. Y. Chen, N. Dorey and K. Okamura, “Dyonic giant magnons,” JHEP **0609** (2006) 024, arXiv:hep-th/0605155.
- [8] J. A. Minahan, A. Tirziu and A. A. Tseytlin, “Infinite spin limit of semiclassical string states,” JHEP **0608** (2006) 049, arXiv:hep-th/0606145.
- [9] V. A. Kazakov, A. Marshakov, J. A. Minahan and K. Zarembo, “Classical / quantum integrability in AdS/CFT,” JHEP **0405** (2004) 024, arXiv:hep-th/0402207.
- [10] N. Beisert, V. A. Kazakov and K. Sakai, “Algebraic curve for the SO(6) sector of AdS/CFT,” arXiv:hep-th/0410253.
- [11] N. Beisert, V. A. Kazakov, K. Sakai and K. Zarembo, “The algebraic curve of classical superstrings on AdS(5) x S\*\*5,” arXiv:hep-th/0502226.
- [12] S. Schafer-Nameki, “The algebraic curve of 1-loop planar N = 4 SYM,” Nucl. Phys. B **714** (2005) 3, arXiv:hep-th/0412254.
- [13] L. F. Alday, G. Arutyunov and A. A. Tseytlin, “On integrability of classical superstrings in AdS(5) x S\*\*5,” JHEP **0507** (2005) 002, arXiv:hep-th/0502240.
- [14] N. Dorey and B. Vicedo, “On the dynamics of finite-gap solutions in classical string theory,” JHEP **0607** (2006) 014, arXiv:hep-th/0601194.
- [15] N. Dorey and B. Vicedo, “A symplectic structure for string theory on integrable backgrounds,” arXiv:hep-th/0606287.
- [16] K. Okamura and R. Suzuki, “A Perspective on Classical Strings from Complex Sine-Gordon Solitons,” arXiv:hep-th/0609026.
- [17] S. Novikov, S. V. Manakov, L. P. Pitaevsky and V. E. Zakharov, *Theory Of Solitons: The Inverse Scattering Method*, New York, Usa: Consultants Bureau (1984)
- [18] E. D. Belokolos, A. I. Bobenko, V. Z. Enol’skii, A. R. Its, V. B. Matveev, *Algebro-Geometric Approach to Nonlinear Integrable Equations*, Springer-Verlag Telos (1994)
- [19] M. Spradlin and A. Volovich, “Dressing the giant magnon,” JHEP **0610** (2006) 012, arXiv:hep-th/0607009.

- [20] C. Kalousios, M. Spradlin and A. Volovich, “Dressing the giant magnon. II,” arXiv:hep-th/0611033.
- [21] B. Vicedo, work in progress.
- [22] G. Arutyunov, S. Frolov and M. Zamaklar, “Finite-size effects from giant magnons,” arXiv:hep-th/0606126.
- [23] P. Griffiths and J. Harris, *Principles of Algebraic Geometry*, John Wiley & Sons, 1978
- [24] P. Byrd and M. Friedman, *Handbook of Elliptic Integrals for Engineers and Scientists* (2nd edition), Springer, 1971
- [25] A. Calini and T. Ivey, “Finite-gap Solutions of the Vortex Filament Equation, I” arXiv:nlin.SI/0411065.